1st AIAA Atmospheric and Space Environments Conference
22 - 25 June 2009, San Antonio, Texas

AIAA 2009-4264

Experimental Study of Full-Scale Iced-Airfoil Aerodynamic Performance using Sub-scale Simulations

Greg T. Busch* and Michael B. Bragg†
University of Illinois, Urbana, IL 61801

Recent research in sub-scale ice accretion aerodynamic simulation and the current state of understanding in this area are reviewed. The flowfields and defining aerodynamic characteristics of the main types of ice accretion are discussed: ice roughness, streamwise ice, horn ice, and spanwise-ridge ice. Reynolds number effects are found to be small in many cases, but additional data are needed for certain types of accretion from Re = 2.0 x 10^6 – 5.0 x 10^6. Uncertainties in representing ice accretion geometry are substantial and in many cases may cause differences in aerodynamic performance on the order of the differences observed between a sub-scale simulation and the corresponding accretion. It is found that directly scaling roughness height on ice roughness, streamwise ice, and short-ridge ice simulations tends to produce conservative estimates of aerodynamic performance. Surface roughness is not usually necessary to accurately represent horn-ice simulations but improves the fidelity of tall-ridge simulations.

Nomenclature

α	angle of attack
c	chord length
C_d	drag coefficient
$C_{d,min}$	minimum drag coefficient
C_l	lift coefficient
$C_{l,max}$	maximum lift coefficient
C_m	pitching-moment coefficient about the quarter-chord
C_p	pressure coefficient
k	feature height
M	freestream Mach number
Re	freestream Reynolds number, based on the airfoil chord length
s	airfoil model coordinate along the surface length
θ	ice-shape horn or ridge angle with respect to the airfoil chordline
x	coordinate in the airfoil model chordwise direction

Introduction

The effects of ice accretion on aircraft surfaces can substantially reduce aircraft performance, especially if the wing or control surfaces are affected. Reductions in airfoil maximum lift of over 50% and increases in $C_{d,min}$ of more than 400% have been observed for some types of ice accretion.[1] It is important to determine the aerodynamic performance penalties that can be expected from a given icing encounter so that aircraft can be certified for flight through icing conditions. These penalties are often determined experimentally using aerodynamic wind tunnels, as flight testing is difficult and expensive and CFD methods typically lack the desired accuracy, especially in highly separated, unsteady flows near $C_{l,max}$. However, measuring iced-airfoil performance in an aerodynamic wind tunnel requires construction of a sub-scale geometric representation of an ice accretion, referred to as a sub-scale simulation, as icing tunnels are unsuitable for obtaining aerodynamic performance data. Recently, a major research program developed methods of categorizing and simulating ice accretion on wind tunnel airfoil models.[2] Four types of ice accretion were identified and classified based on key flowfield features,[3] and methods of constructing sub-scale simulations for each of these types of accretion have been developed.

* Graduate Research Assistant, Department of Aerospace Engineering, Member AIAA.
† Professor of Aerospace Engineering, Executive Associate Dean for Academic Affairs, Fellow AIAA.

Bragg et al.[3] have characterized four main types of airfoil ice accretion based on key geometric and aerodynamic characteristics: ice roughness, streamwise ice, horn ice, and spanwise-ridge ice. Ice roughness is generally higher than the local boundary layer thickness, so each roughness element can be analyzed as an isolated flow obstacle in regions where the concentration is low. If the Reynolds number based on roughness height, Re_k, is sufficiently high, the roughness element will cause the boundary layer to undergo bypass transition, a process which is much slower and less energetic than natural transition.[4] This alters the boundary layer development relative to natural transition and generally results in premature boundary layer separation near the trailing-edge of the airfoil. Streamwise ice also has surface roughness and ice feathers which affect boundary-layer development in a similar manner to ice roughness. Additionally, slope discontinuities at the ice/airfoil junction may cause a short separation bubble to form. Short bubbles have only a local effect on the airfoil flowfield and do not grow significantly with angle of attack, but their position on the airfoil may change slightly with changes in angle of attack. The horn-ice accretion flowfield has much in common with that of a backward facing step. The tip of the horn generates a strong adverse pressure gradient which triggers boundary layer separation at a fixed point independent of angle of attack, and a shear layer forms between the inviscid flow over the top of the horn and the recirculatory flow behind the horn. The shear layer entrains high energy flow from the inviscid region and eventually reattaches to the airfoil (if the airfoil is at sufficiently low angle of attack), forming a long separation bubble. The separation bubble dominates the flowfield and usually causes thin-airfoil stall. For the fourth type of ice accretion, spanwise-ridge ice, the boundary layer has time to develop before separation occurs, and may even transition upstream of the ridge. In this sense, the ridge acts as a flow obstacle. As with horn ice, the strong adverse pressure gradient at the tip of the ridge causes a separation bubble to form and the type of separation bubble determines whether the ridge is considered to be tall or short.

Based on these key flowfield characteristics and existing performance data obtained using ice accretion simulations, Bragg et al.[3] identified important geometric features on each type of accretion. For ice accretions with long separation bubbles, such as horn-ice and spanwise-ridge ice, it was observed that geometric intricacies and surface roughness were not as important to represent as was the gross ice geometry. For smaller, more conformal types of accretion in which the dominant mechanism for affecting airfoil performance is alteration of the boundary layer, it was observed that changes in surface roughness height, concentration, and chordwise extent were important. These conclusions suggest that a simulation which appropriately represented the important geometric features of an accretion would cause similar performance penalties, as long as Reynolds and Mach number effects were small or the parameters kept constant. However, little data was available on full-scale iced airfoils to quantify the accuracy with which simulations could reproduce full-scale iced-airfoil aerodynamics.

Broeren et al.[5] recently obtained aerodynamic performance data on high-fidelity, full-scale ice accretion castings for each of the four types of ice accretion at Reynolds numbers between 4.6×10^6 and 16.0×10^6 and Mach numbers between 0.10 and 0.28 using a NACA 23012 airfoil model. It was found that the effects of Reynolds and Mach number on iced-airfoil performance were small, confirming previous work investigating these effects. This conclusion and the observations of Bragg et al. suggested that sub-scale simulations could accurately reproduce the effects of a full-scale accretion if designed appropriately.

The study by Broeren et al.[5] provides a set of aerodynamic performance data representative of that which would be obtained in flight conditions and can be used as a baseline with which to compare data obtained from sub-scale simulations to quantify the accuracy of simulation methods. Busch et al.[6] incorporated suggestions made by Bragg et al.[3] regarding important geometric features in the design of sub-scale simulations of the accretions studied by Broeren et al.[5] The airfoil performance degradation caused by these sub-scale simulations at low Reynolds number was compared with the full-scale, high Reynolds number data of Broeren et al. to quantify the accuracy of the simulation methods. Good agreement was observed for accretions for which a large separation bubble dominated the flowfield. Agreement was not as good for simulations for which Bragg et al. suggested surface roughness to be important, and this will be discussed later in this paper.

The purpose of this paper is to provide a summary of recent research conducted to develop a methodology for simulating full-scale iced-airfoil aerodynamics using sub-scale ice accretion simulation methods and to explain the current state of understanding in this area. The paper addresses some of the issues inherent in sub-scale ice accretion simulation and, for each type of ice accretion, discusses which features are important to accurately represent on a sub-scale simulation in order to closely reproduce the full-scale iced-airfoil performance and what type of accuracy can be expected from different types of simulation.

Issues in Sub-scale Ice Accretion Simulation

Iced-airfoil aerodynamic performance is not usually measured in icing wind tunnels due to instrumentation difficulties, icing cloud non-uniformity, and high freestream turbulence levels. It is difficult to obtain C_l and C_m data from surface static pressure taps, as taps can not be easily installed in the ice accretion. A force balance can not usually be used accurately, as the icing cloud in icing tunnels tends to be concentrated near the center of the test section, resulting in ice accretions which taper off near the walls. Even if these problems are overcome, icing tunnels usually have high freestream turbulence levels to enhance mixing and promote icing cloud uniformity, a characteristic which is undesirable when obtaining performance measurements. Because of these limitations, iced-airfoil performance is usually measured in aerodynamic wind tunnels, which requires that an ice accretion simulation be constructed.

To perfectly simulate an ice accretion, one should match Reynolds and Mach numbers and build a simulation of identical geometry to the airfoil plus accretion. While the resulting simulation would no doubt reproduce the iced-airfoil aerodynamic performance very accurately, it would be extremely expensive to produce and test. To reduce costs, and since full-scale facilities may not be available, it is usually necessary to use sub-scale airfoil models. This requires that the ice accretion geometry also be scaled. Frequently, it is very difficult and expensive to document every feature of an accretion, so some of the detail is lost in the documentation process. Even if every feature could be documented, some detail may be lost while fabricating and scaling the simulation. Another tool frequently used to design sub-scale ice simulations is the LEWICE ice accretion prediction code, which can predict gross 2-D ice geometries on airfoils.[7] However, the code does not predict surface roughness or feather formation. As a result of the inability to exactly represent ice accretion geometry, sub-scale ice simulations usually have much simpler geometries than the accretions they represent. In addition to the difficulties inherent in reproducing ice accretion geometry, it is also expensive to match both Reynolds and Mach number on a sub-scale simulation as matching both of these parameters requires a pressure tunnel. Atmospheric tunnels are generally used, so only Mach number or Reynolds number can be matched. Several studies have looked at the effects of varying Reynolds and Mach number on airfoil performance, and these studies are discussed next.

Reynolds and Mach number effects on Iced-Airfoil Performance

Reynolds and Mach number effects on clean airfoil performance can be substantial. Typically, $C_{l,max}$ increases as Re increases and decreases as M increases up to about 0.3, but it has been shown that these effects are much less significant on iced airfoils. In Fig. 1(a), the effects of changing Re on $C_{l,max}$ are shown for several airfoils at constant M, and in Fig. 1(b) the effects of changing M at constant Re are shown. In Fig. 1(a), line color and pattern denote the Mach number of the corresponding data set (kept constant) while Re was varied, and in Fig. 1(b) the line color and pattern denote the Reynolds number (kept constant) while M was varied. Symbol type denotes the airfoil configuration (clean or iced) and if iced, what type of ice accretion/simulation was present.

In Fig. 1(a), the trend of increasing $C_{l,max}$ with increasing Re (at constant M) on clean airfoils (closed symbols) is clear in most cases. In contrast, the $C_{l,max}$ of most iced airfoils exhibits insensitivity to changes in Re, with a few exceptions. The figure shows that two particular ice roughness simulations (using k/c = 0.0002 and 0.0006 sandpaper roughness) had $C_{l,max}$ increase by about 0.1 from Re = 2 x 10^6 – 3.5 x 10^6. Beyond Re = 3.5 x 10^6, all roughness simulations showed insensitivity to changes in Re. Papadakis and Gile Laflin[32] measured Re effects below Re = 2.0 x 10^6 on $C_{l,max}$ of airfoils with different sandpaper roughness heights and found that Re effects were significant, though no clear trends were evident. More data are needed below Re = 3.5 x 10^6 (especially above Re = 2.0 x 10^6) on ice roughness simulations to determine the extent to which Re effects are significant. Streamwise ice accretions, for which surface roughness has a similar effect as on ice roughness accretions, may also show some degree of Reynolds number sensitivity, but little data are available in this range of Re. Also in Fig. 1(a) is a ridge simulation (a short ridge) in Fig. 1(a) with $C_{l,max}$ near 1.5 which shows some sensitivity to variations in Re (at two different values of M), but no clear trend. Similar to the trends for ice roughness accretions, Re effects have been shown to be significant below Re = 1.7 x 10^6 for short ridge ice accretions.[8]

The effect of Mach number on iced airfoil $C_{l,max}$ over the range of Mach numbers shown is in general larger than the effect of Re. Most showed a slight decrease in $C_{l,max}$ as Mach number increased, although the changes were generally not as drastic as with the clean airfoil. Also, changes in $C_{l,max}$ with varying Mach number were usually much smaller than the degradation in performance due to the presence of ice. For sub-scale simulation purposes, the trends in Reynolds and Mach number are fortunate, as Mach numbers of 0.2 and Reynolds numbers close to 2.0 x 10^6 can usually be achieved at reasonable cost so most types of accretion can be simulated at sub-scale with

confidence. As discussed above, more data are needed for ice roughness and short spanwise ridges at Reynolds numbers between 2.0 x 10^6 - 3.5 x 10^6, as little data exists in this range for these types of accretion.

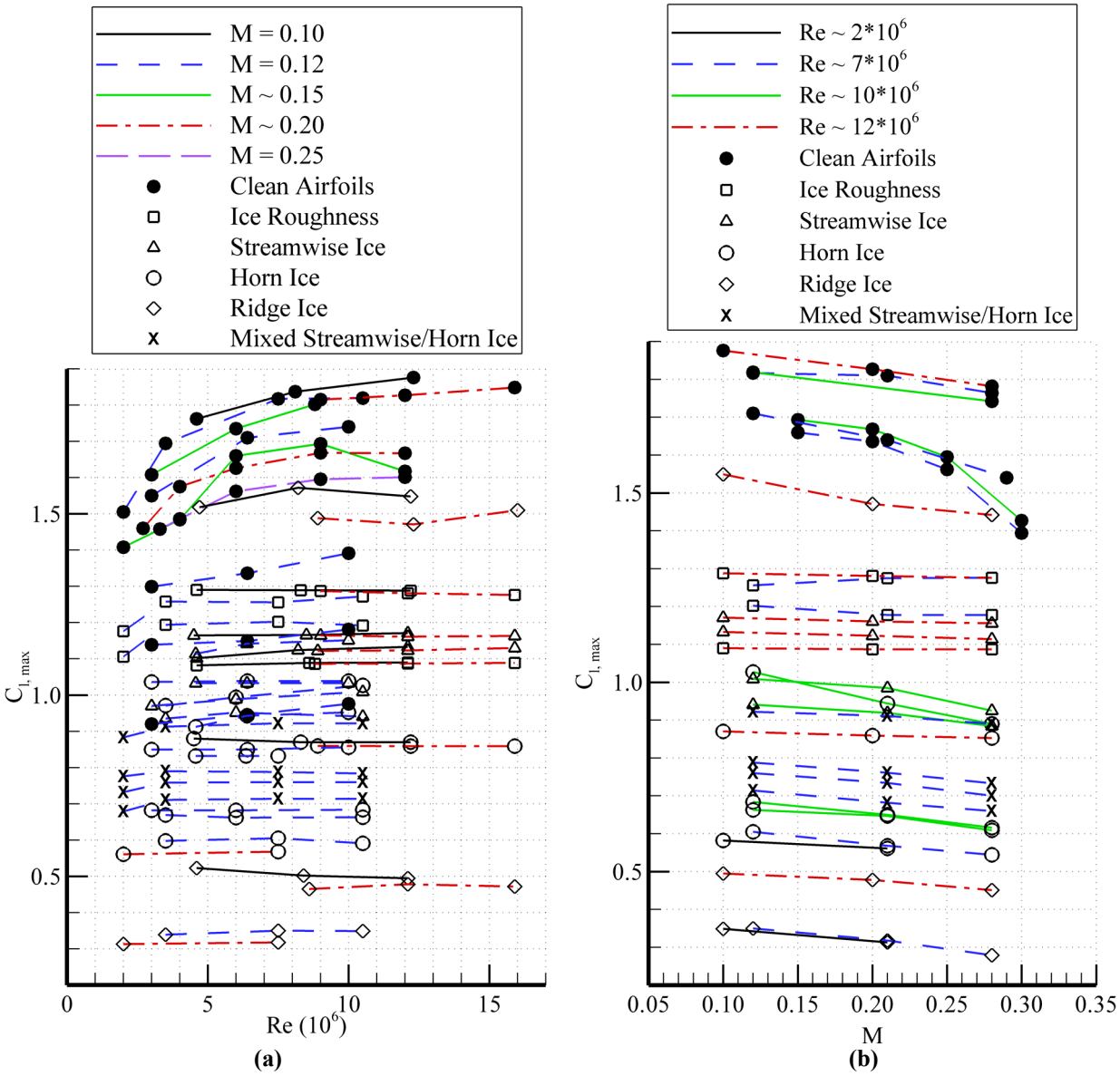

Fig. 1 Effect of (a) Reynolds number at constant M and (b) Mach number at constant Re on $C_{l,max}$ for different types of ice accretion. Data from references 5, 9, 10, 11, 17, and 18.

Ice accretion geometry uncertainty

As discussed earlier, icing tunnels are not ideal for determining iced-airfoil aerodynamic performance so aerodynamic tunnels are usually used for this purpose. This requires that simulations of the ice accretion be constructed, and this process may introduce uncertainty into the performance measurements, depending on the type of simulation used. The highest fidelity simulation commonly used is a casting. Castings are usually constructed from molds of ice accreted in an icing wind tunnel. They capture nearly all of the three-dimensional geometry of the accretion, including surface roughness, and are considered to give the "true" aerodynamic penalties associated with the ice accretion. However, the fabrication of castings requires time in an icing wind tunnel and an icing wind tunnel model of a similar scale to the aerodynamic model that will be used. Since aerodynamic models are generally

of a smaller scale than the airfoil they represent, this may require scaling of icing conditions. Such scaling is not validated to reproduce ice feathers of the same height k/c as would be accreted on a full-scale icing model.[12,13]

These constraints regarding the use of castings demonstrate the need for simpler, more easily scaled simulations. Two such examples are 2-D smooth and simple-geometry simulations. 2-D smooth simulations are based on tracings of an iced-airfoil cross-section. The cross-section is extruded along the airfoil span to create a constant cross-section, two-dimensional simulation (the ice tracing is frequently smoothed prior to simulation construction). Simple-geometry simulations are also based on tracings of the ice accretion, but use simple-geometric shapes to capture only the main geometric features of the ice accretion rather than trying to duplicate the tracing exactly. This lowers their cost and makes them ideal for use in parametric studies. Simple-geometry simulations are considered to be of a lower geometric fidelity than 2-D smooth simulations. Surface roughness is frequently added to both 2-D smooth and simple-geometry simulations to increase simulation fidelity.

To construct sub-scale 2-D smooth and simple-geometry simulations, ice accretions are usually geometrically-scaled (constant k/c) to create sub-scale simulations. This has worked well in simulating large accretions. Geometric-scaling has been less successful in simulating small accretions or accretions in which surface roughness is important, as important geometric features may be on the order of the height of the local boundary layer. Whalen[14,15] constructed sub-scale simulations of ridge-ice using boundary-layer scaled (constant k/δ) geometries in addition to geometrically-scaled geometries. The boundary-layer scaled geometries were much larger than the geometrically-scaled geometries, and tended to cause increased aerodynamic penalties relative to those of the geometrically-scaled simulations. Broeren et al.[9] showed that the geometrically-scaled simulations were likely already too conservative, and that other scaling methods may be necessary to appropriately scale ice geometries which have heights that may be on the order of the local boundary-layer thickness at relevant lift coefficients. However, most simulations to date, including those discussed in this paper, have been designed using geometric scaling procedures.

Some studies have used different types of simulations of the same type of accretion and compared the differences in aerodynamic performance degradation. For example, Gurbacki[16] compared 2-D smooth simulations with and without grit roughness to corresponding castings of horn and streamwise-ice accretions. It was found that the 2-D smooth simulation had a lower $C_{l,max}$ than the casting for the horn ice, but the casting had a lower $C_{l,max}$ for the streamwise ice. Another study by Addy and Chung[17] comparing a horn-ice casting and its 2-D smooth simulation on an NLF-0414 found that the 2-D smooth simulation had a higher $C_{l,max}$ than the casting. Yet another study by Addy et al.[18] on a business jet airfoil found the 2-D smooth simulation to have a lower $C_{l,max}$ than the casting.

The discrepancies observed in these studies prompted an investigation into the use of ice accretion tracings used to design 2-D smooth simulations.[19] Most ice accretions have some variation in geometry along the airfoil span. Therefore, tracings taken at different locations along the span will differ. These tracings are used to design 2-D smooth simulations, so the geometry of a 2-D smooth simulation constructed from a tracing taken at one spanwise station will differ from one constructed from a tracing taken at a different spanwise station. Blumenthal et al.[19] quantified the differences in aerodynamic performance resulting from these variations (shown in Fig. 2) using a NACA 0012 airfoil model. A 2-D smooth simulation was constructed with interchangeable horn geometries. The aerodynamic performance of the NACA 23012 with three upper surface horns, representative of various cross-sections of the horn along the airfoil span, was measured and compared with the casting on which the simulation was based. It was found that variations in horn height of 11% and 26% resulted in variations in $C_{l,max}$ of 7% and 13%, respectively (Fig. 3). Iced-airfoil C_d also changed markedly, with $C_{d,min}$ of the shortest horn being 14% lower than C_d of the tallest horn. These results indicate that it is important that ice accretion tracings used to construct 2-D smooth simulations be taken at a spanwise station which is representative of the overall horn geometry.

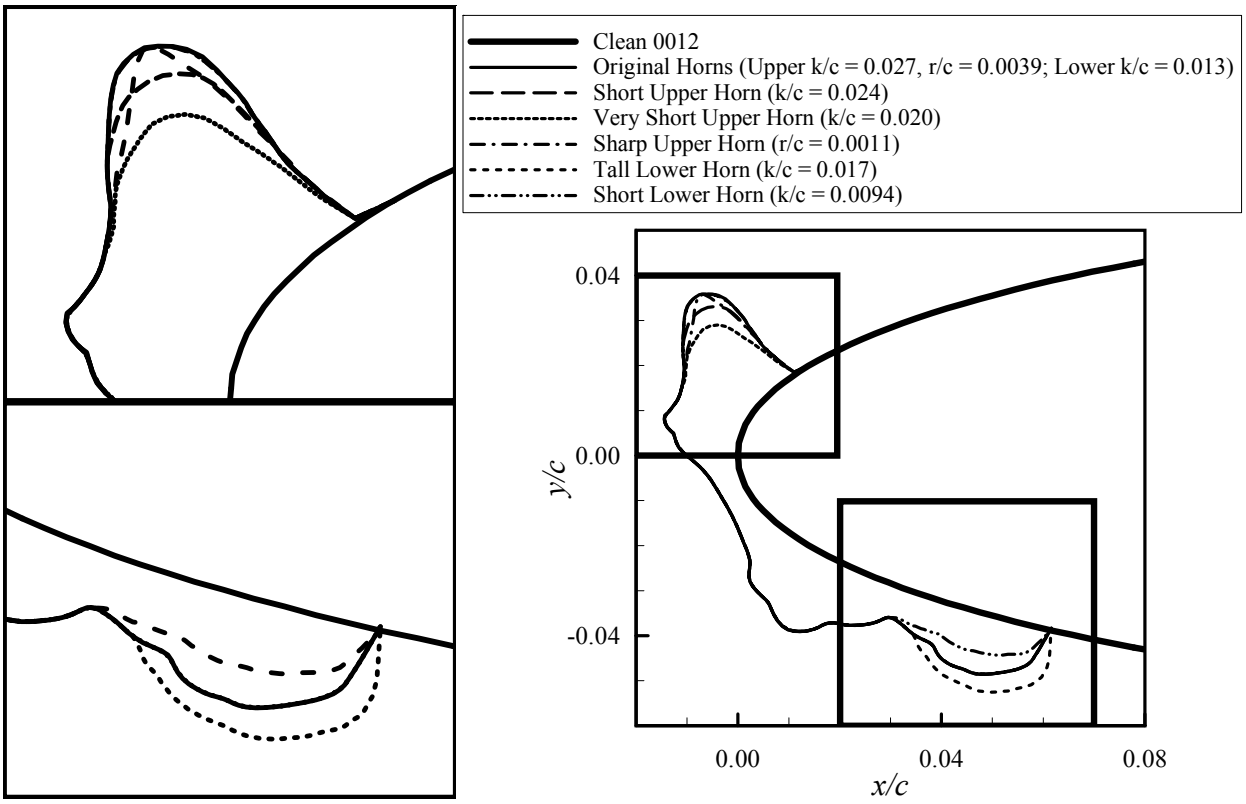

Fig. 2 Example of the variation in ice geometry that may result from taking tracings at different spanwise stations. [19]

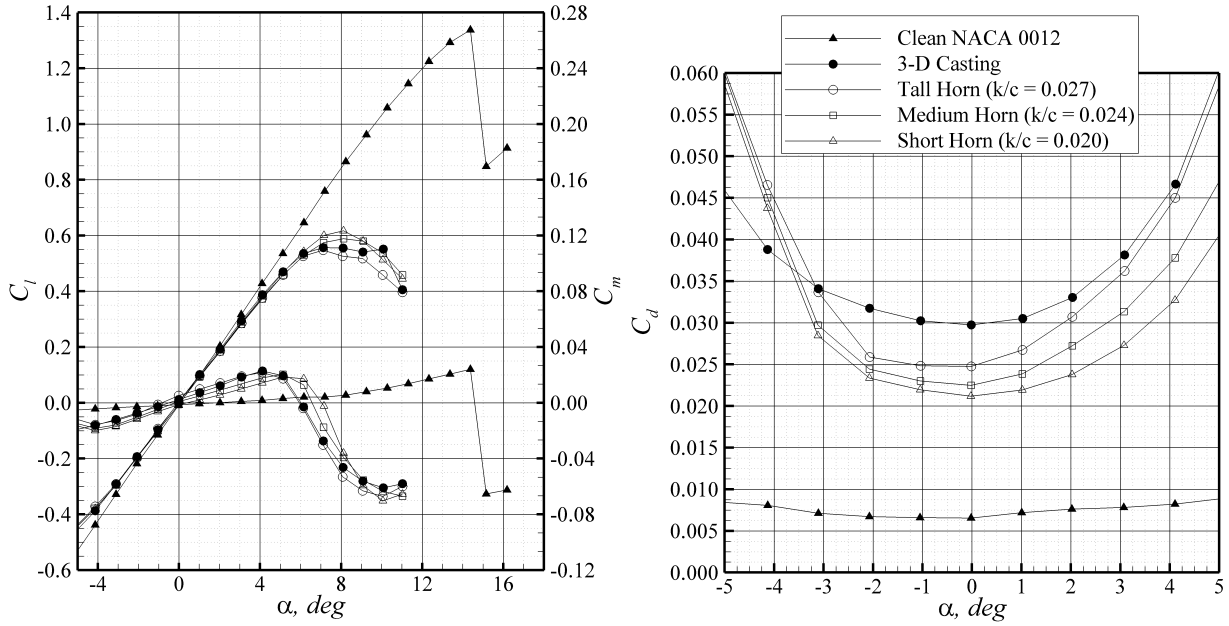

Fig. 3 Effects of minor variations in upper-surface horn geometry which may result from different tracing locations on C_l, C_m, and C_d of a NACA 0012 airfoil.[19]

Jackson[20] performed a similar study on the effects of tracing location on the aerodynamic performance of 2-D smooth simulations on a NLF-0414 airfoil. An accretion was traced at three spanwise stations located 6 inches

apart, and a 2-D smooth simulation was produced from each tracing. A fourth 2-D smooth simulation was constructed using a LEWICE predicted ice geometry. The cross-sections of each of these 2-D smooth simulations are shown in Fig. 4. Variations in $C_{l,max}$ on the order of 18% were observed, with the $C_{l,max}$ of the LEWICE simulation bracketed by the other simulations. $C_{d,min}$ of the simulation based on the 30-inch station tracing was double that of the 42-inch station tracing, and C_d of the LEWICE simulation was in between these two simulations at positive angles of attack. These results agree with those of Blumenthal et al.[19] in suggesting that the selection of tracing location may have a substantial affect on aerodynamic performance and therefore must be chosen carefully to successfully simulate an ice accretion.

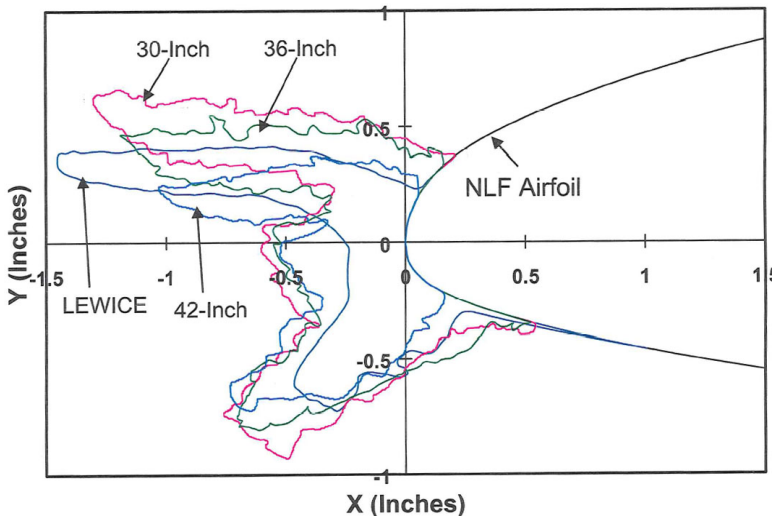

Fig. 4 Cross-sections of four 2-D smooth simulations investigated by Jackson.[20] Three of the simulations were based on tracings of an ice accretion, and the fourth was based on LEWICE.

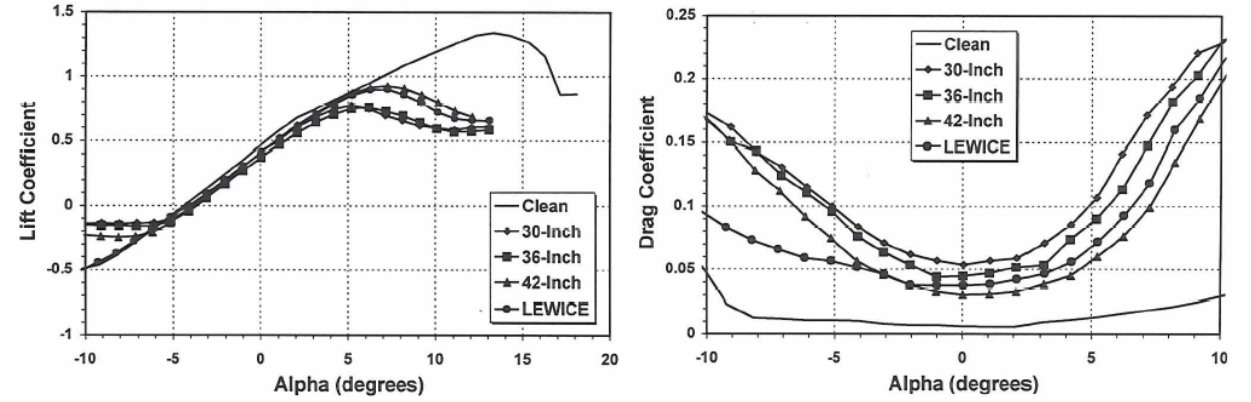

Fig. 5 Comparison of aerodynamic performance among the four 2-D smooth simulations investigated by Jackson. Re = 1.8 x 10^6, M = 0.18.[20]

In addition to the effects of tracing location, another source of uncertainty regarding the geometry of ice accretion simulations comes from the inability of icing tunnels to exactly reproduce icing conditions and therefore ice accretion geometry. Thus, there is some variation from run to run in ice accretion geometry under nominally identical icing conditions. This variation has been documented in several earlier studies,[21,22,23,24] and may be on the order of the variation in ice geometry along the airfoil span. Examples of the repeatability of ice accreted in the Icing Research Tunnel at NASA Glenn are shown in Fig. 6 for horn and streamwise-ice accretions. For the horn-ice, upper-surface horn height and angle changed slightly from run to run. Based on the data taken by Blumenthal et al. and Jackson discussed above and shown in Fig. 2 - Fig. 5, these variations would likely have a notable effect on iced-airfoil aerodynamic performance. This should be considered when viewing ice simulation data, as the

differences in aerodynamic performance between a simulation and corresponding accretion are frequently on the order of differences which may result from different icing encounters in nominally identical icing conditions.

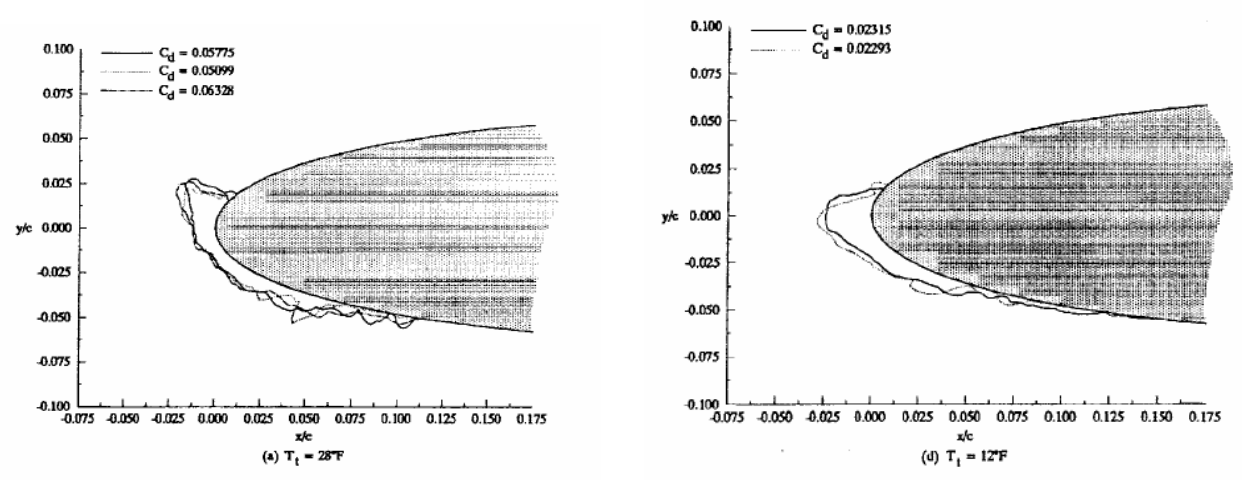

Fig. 6 Representative ice accretion repeatability in the NASA Glenn Icing Research Tunnel for (a) horn ice and (b) streamwise ice.[21]

Iced-airfoil performance measurement uncertainty

Once an ice accretion simulation is constructed, it is usually instrumented with pressure taps so that lift and pitching moment may be measured. However, unlike a clean airfoil, which has a smooth, continuous surface, the ice accretion geometry is highly irregular. It is important to select pressure tap locations which will give representative measurements of the pressure around the simulation. Blumenthal[25] investigated the effect of pressure tap placement, and also the effects of different types of instrumentation. The two methods that were explored were the installation of pressure taps directly in a casting (Fig. 7(a)) and the use of a thin, two-dimensional profile of the simulation geometry, known as a pressure slice, in which to install the pressure taps (Fig. 7(b)). Blumenthal discussed that localized high points on the ice accretion generally correspond to regions of flow acceleration, so a pressure tap located at such a point would read a lower pressure than a tap placed nearby. Similarly, a pressure tap located immediately in front of an ice feather or roughness element may measure a higher pressure than a tap placed on top of the element. Of course, if the simulation is instrumented with a large number of pressure taps, these effects are less important, but the complex geometry of most simulations restricts the number of pressure taps that may be practically installed. Blumenthal carefully selected tap locations for both tapped casting and pressure slice configurations of horn and streamwise-ice accretions such that the integrated effects would balance out. For the horn-ice simulations, both the tapped-casting and pressure-slice methods yielded similar integrated performance data. For the streamwise-ice simulations, ice feathers were found to have a notable effect on the C_p distribution on the upper surface of the simulation; Fig. 7 shows areas of localized higher pressure measured at taps which were located directly in front of feathers on the tapped casting or local maximums of the pressure slice geometry. These fluctuations did not have a large effect on the downstream pressure distributions until just prior to stall. At high angles of attack, the differences in the C_p distributions corresponded to slightly lower values of C_l and C_m measured using the pressure-slice method compared with those measured using the tapped casting method..

While iced-airfoil C_l and C_m are often obtained using surface static pressure taps, iced-airfoil C_d is generally measured using a wake rake and standard momentum-deficit methods and is not as affected by pressure tap placement. However, it has been found that the spanwise position of the wake rake behind an ice simulation may have a large effect on the measured value of C_d, even on 2-D simulations. Busch et al.[26] reported variations in C_d of 32% at α = 0 deg. for a horn-ice casting, but found that the variation diminished to 11 % at α = 4 deg. (Fig. 8(a)). For a 2-D simple-geometry simulation of the same horn-ice accretion, C_d varied by 20% at α = 0 deg. and by 5% at α = 4 deg. Blumenthal[25] measured variations of up to 16% for horn-ice and 25% for streamwise-ice castings at α = 0 deg. The local increase in C_d in the case of castings appears to correlate loosely with increases in separation bubble size, but not directly with upper surface horn geometry. Further testing by the authors on ice roughness simple-geometry simulations have shown variations in C_d of 45% and 20% at α = 0 deg. and 10 deg., respectively, when measured at different spanwise stations (Fig. 8(b)). It is also interesting that variations of over 15% have been observed for clean airfoils at low Reynolds numbers by Guglielmo,[27] Althaus,[28] and the current authors. These

results indicate that to obtain accurate measurements of C_d, wake surveys should be taken at multiple spanwise stations and averaged. Unfortunately, time and cost constraints frequently prohibit such measurements.

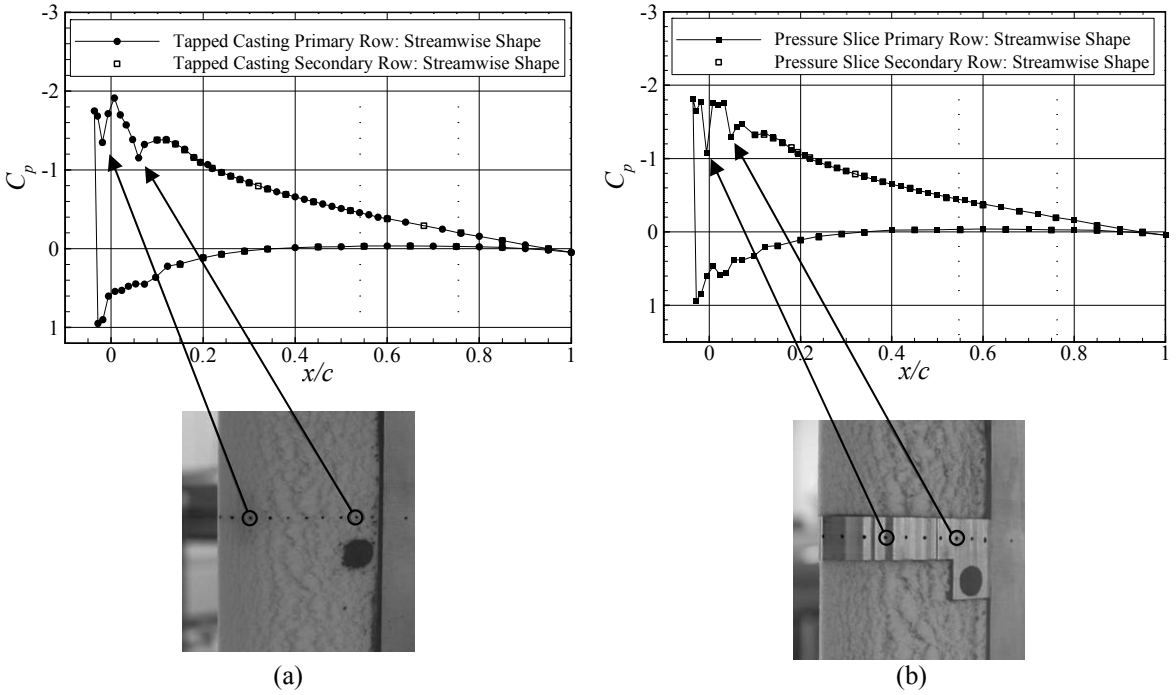

(a) (b)

Fig. 7 Measured surface pressure distributions for a NACA 23012 airfoil with streamwise-ice castings instrumented with (a) pressure taps drilled directly into the surface and (b) a 2-D pressure slice.[19]

As with most other types of wind tunnel testing, one other issue that affects aerodynamic performance measurements relates to tunnel interference. There are three corrections which must be applied to measurements obtained in a wind tunnel to extrapolate the 2-D data to free-flight conditions: solid blockage, wake blockage, and streamline curvature. Solid blockage refers to the reduction in test section area caused by the presence of the airfoil and ice simulation. Wake blockage refers to the reduction of flow velocity in the wake of the model. Both of these effects cause an increase in the effective freestream velocity near the airfoil model. Streamline curvature effects result from the presence of the tunnel walls, which prevent the streamlines from achieving the same paths as would be achieved in free flight. This causes an effective increase in airfoil camber which artificially increases the airfoil C_l and C_d. Corrections for each of these effects are usually applied to aerodynamic performance measurements, but these corrections generally tend to be approximate and likely do not exactly yield the aerodynamic performance that would be measured in free flight.

Considerations for Designing Sub-scale Simulations

Ice accretion on an airfoil affects the flowfield predominantly in two ways: the gross ice geometry may substantially alter the inviscid flowfield and surface roughness may affect boundary-layer development. With regard to the classifications of ice shapes defined by Bragg et al.,[3] horn-ice and spanwise-ridge ice affect the flowfield predominantly through the former mechanism, and ice roughness and streamwise-ice mainly through the latter. There may be, of course, significant interaction between these two mechanisms, but for the purposes of simulation it is convenient to consider this difference.

Ice accretions which substantially alter the inviscid flowfield usually do so through the generation of a long separation bubble, as discussed in the Introduction. This separation bubble results from ice geometry which causes a severe adverse pressure gradient far from the clean airfoil surface relative to the boundary-layer height. For these accretions, the separation point does not move significantly with changes in angle of attack, Mach, or Reynolds numbers.[29] These types of shapes may have a high degree of surface roughness that may affect boundary-layer development upstream of the separation point, but the roughness does not significantly affect the location of the separation point. Roughness downstream of the separation point is usually located in a separation bubble and also

has a relatively small effect on the iced-airfoil flowfield; this is discussed in more detail in the Horn Ice section of this paper.

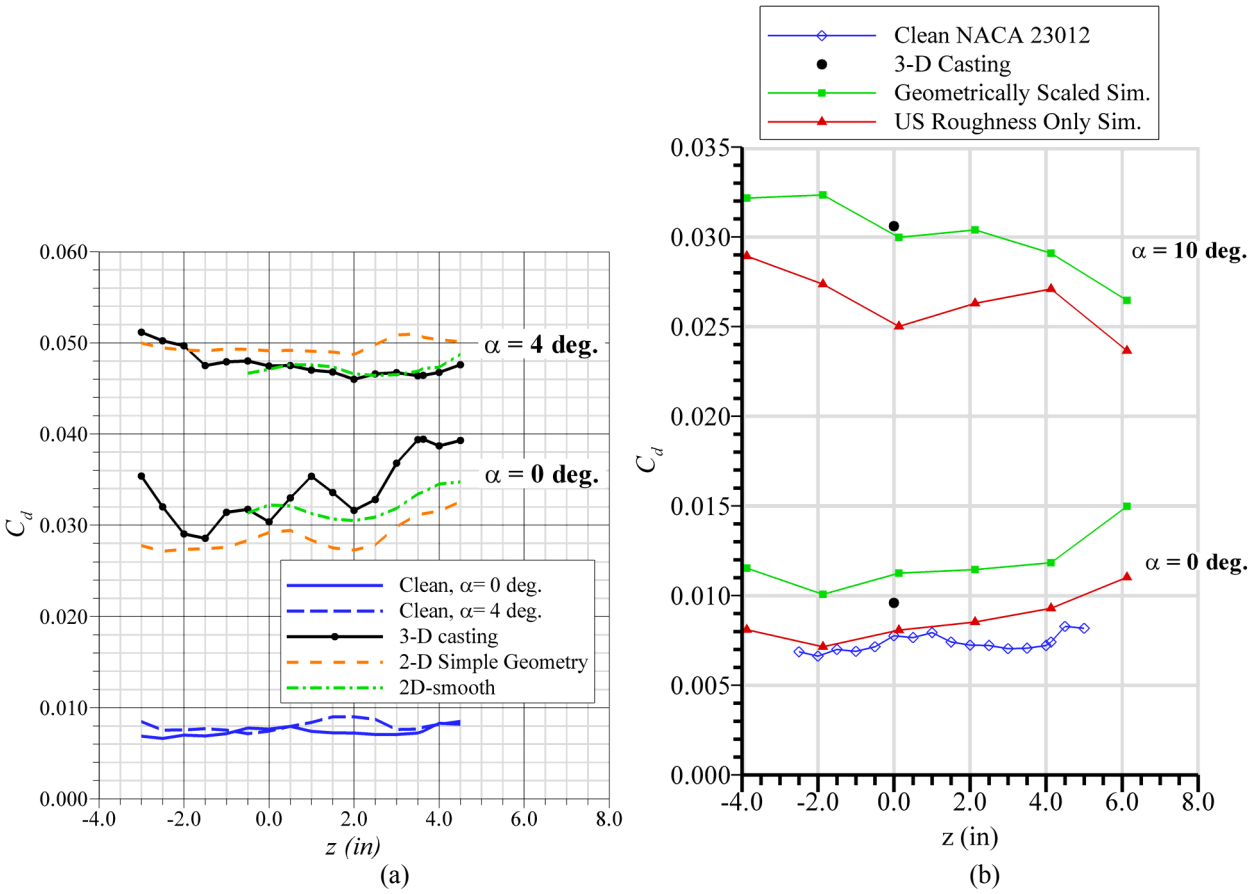

Fig. 8 Variation in C_d measured at different spanwise stations behind a NACA 23012 airfoil with (a) horn-ice and (b) ice roughness simulations. C_d for the ice roughness casting in (b) was measured in a different wind tunnel at only one spanwise station and is represented by a single point at z = 0.0 in..[26]

Ice accretions which affect the iced-airfoil flowfield by altering boundary-layer development usually have gross ice geometries which do not generate long separation bubbles, although they may cause short separation bubbles. Short bubbles are stable and do not grow significantly with angle of attack, and they have only a local effect on the airfoil pressure distribution. For these types of accretion, the effects of surface roughness dominate. The roughness extracts momentum and reduces boundary-layer health compared to the clean airfoil, causing it to separate early. This causes trailing-edge separation to occur at lower angle of attack than for the clean airfoil, and results in trailing-edge stall. In general, roughness of larger size and higher concentration (to a point) causes more severe aerodynamic penalties; this is discussed in the ensuing Ice Roughness and Streamwise Ice sections.

The relative effects of surface roughness and gross ice geometry varies by accretion type and must be considered when designing ice accretion simulations. Considerations for each type of accretion are now discussed.

Ice Roughness

Ice roughness often results from the initial accumulation of ice on an airfoil before a larger geometry has had time to form. Because ice roughness has no large-scale ice geometry, it is usually represented by applying grit roughness to a clean airfoil model to construct a simple-geometry simulation. The roughness can be characterized predominantly by its height, concentration, and chordwise location and extent. The effects of ice roughness on the airfoil flowfield come mainly through alteration of the airfoil boundary layer, and each of these parameters can affect the magnitude of this alteration. The aerodynamic effects of variations in these parameters are discussed by Bragg et al.[3] and are elaborated on further in this section.

Important geometric features

Bragg et al.[3] discuss a study by Brumby[30] which examined the effect of average roughness height on aerodynamic performance. Brumby assembled data on NACA airfoils to show the effect of roughness height and location on $C_{l,max}$ (Fig. 9). The trendlines on Brumby's plot show that as roughness height increases, $C_{l,max}$ decreases for a narrow strip of roughness at a given location. Also, as the strip of roughness moves farther aft on the airfoil surface, it has less of an effect on $C_{l,max}$. In Fig. 9, recent ice roughness simulation data for NACA 23012, NLF-0414, and 63_A213 airfoils has been added to Brumby's plot. Roughness on the NACA 23012 airfoil tends to cause larger degradations in $C_{l,max}$ than the trendline would suggest. This is not surprising, as the roughness on the NACA 23012 extended from x/c = 0.00 to x/c = 0.03, whereas the roughness Brumby refers to was only a narrow, localized strip. Brumby[31] mentions unpublished data in which slight roughness extending to x/c = 0.07 on the upper and lower surfaces caused $C_{l,max}$ degradation closer to that which would be caused by an entirely roughened upper surface. Roughness on the NACA 23012 also causes larger performance degradations than roughness of the same height on either the NLF-0414 or modified 63_A213 airfoils; again, this is not surprising, as the NACA 23012's large suction peak near the leading edge makes it particularly sensitive to ice contamination. The NLF-0414, which has only a very mild adverse pressure gradient in the same region, shows much less sensitivity than the NACA airfoils for which Brumby compiled data.

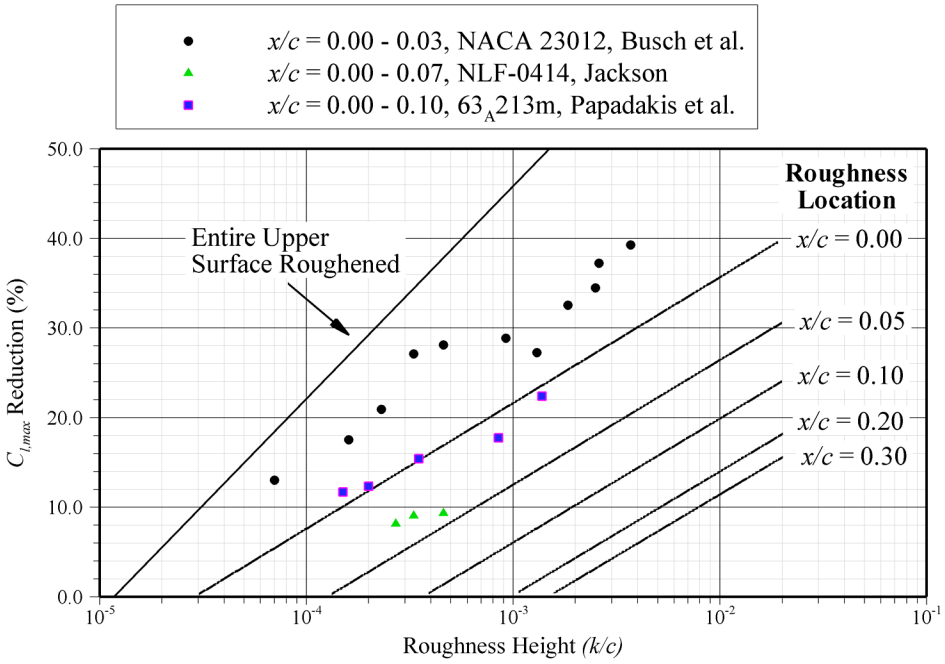

Fig. 9 Effect of roughness height and location on magnitude of $C_{l,max}$ degradation, adapted from Brumby,[30] Busch et al.,[6] Jackson,[20] and Papadakis et al.[32]

Another characteristic used to define ice roughness is its concentration, or area density, which is defined in this paper as the ratio of the area of all individual roughness elements over the total airfoil surface area of the region. On most ice roughness accretions, the stagnation region remains relatively smooth, with large, densely packed regions of roughness on either side. The ice roughness height and concentration generally tend to taper off towards the aft sections of the roughness. Jackson[20] showed that concentration can have a substantial effect on the magnitude of the aerodynamic performance degradation for a NLF-0414 airfoil, and that $C_{l,max}$ is especially sensitive to changes when the roughness concentration is low (Fig. 10). At some critical roughness concentration, which appears to be dependent on roughness height, $C_{l,max}$ becomes insensitive to further increases in concentration. This occurs at about 20% concentration for k/c= 0.00046 roughness and 30% concentration for k/c = 0.0027 roughness extending from x/c = 0 to 7% on the upper and lower surfaces of a NLF-0414 airfoil. Recently, Busch et al.[6] acquired additional data on the effects of roughness concentration for a NACA 23012 airfoil with k/c = 0.00184 roughness extending from x/c = 0.000 – 0.026 on the upper surface and from x/c = 0.004 – 0.041 on the lower surface. These data are co-plotted with Jackson's data in Fig. 10. As would be expected, the larger roughness caused a much larger

degradation in $C_{l,max}$ at a given concentration. This effect is exaggerated even further because the NACA 23012 airfoil geometry is much more sensitive to ice contamination than is the NLF-0414. Despite this much larger decrease in $C_{l,max}$, the trend is consistent with Jackson's data in that there is a critical roughness concentration beyond which further increases in concentration do not have a large effect on $C_{l,max}$.

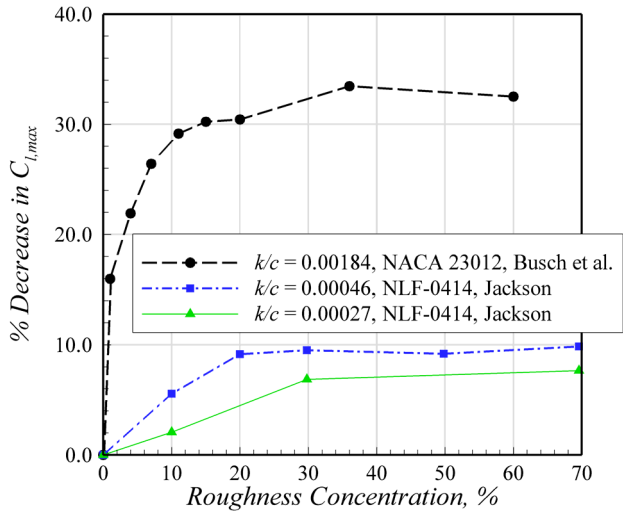

Fig. 10 Effect of roughness concentration as a percent reduction in $C_{l,max}$ between iced and clean NACA 23012 and NLF-0414 airfoils. Data from Busch et al.[6] and Jackson.[20]

Busch et al.[6] briefly investigated the effects of roughness chordwise extents on iced-airfoil performance. It was found that narrow strips of roughness of height k/c = 0.0013 and width s/c = 0.0056 on the upper and lower surface of a NACA 23012 affected C_l and C_m in almost the same way as roughness strips of greater widths of s/c = 0.041 and 0.048 on the upper and lower surfaces, respectively. The wider roughness strips had varying size roughness but with the same maximum height as the narrower strips. The effects of chordwise extent on C_d were notable, as the iced-airfoil C_d with the narrow roughness strips was shifted down by about 0.002 – 0.003 at most angles of attack relative to the ice roughness simulation with larger chordwise extents. Note that in the study of Busch et al., the most upstream location of roughness was the same for both the narrow and wide simulations. Had the locations been different, Fig. 9 suggests that $C_{l,max}$ would likely have been different between the two simulations. Also, according to Fig. 9, it is evident that a much larger increase in chordwise extent would have likely caused a reduction in $C_{l,max}$.

Papadakis et al.[33] used sandpaper roughness of varying grit size and extent to determine the effects of ice roughness on ¼ and full-scale models of a business jet tail at Re = 1.36 x 10^6 and Re = 5.1 x 10^6. Two extents were used: the extents predicted by the LEWICE airfoil ice accretion prediction code (approximately from x/c = 0.017 on the suction surface to x/c = 0.025 on the pressure surface) and from x/c = 0.13 on the suction surface to x/c = 0.13 on the pressure surface. Roughness heights ranged from k/c_{mac} = 0.00026 - 0.00137 on the ¼-scale model and from k/c_{mac} = 0.00009 - 0.00034 on the full-scale model. The effects of roughness extent on aerodynamic performance were small in all cases except for the k/c_{mac} = 0.00137 roughness on the ¼-scale model, where $C_{l,max}$ was about 5% below its value for the shorter roughness extents. Jackson[20] obtained similar results in testing k/c = 0.00046 sandpaper roughness on a NLF-0414. Very little change in $C_{l,max}$ and only a slight change in C_d was documented for chordwise extents from x/c = 0.04 – 0.10 but a notable decrease in $C_{l,max}$ occurred for roughness extending to x/c = 0.29. These results suggest that small changes in roughness extents near the airfoil leading edge usually do not play a large role in affecting airfoil $C_{l,max}$ compared to the effects of roughness height and concentration, but, consistent with Brumby,[30] large changes in roughness extent may reduce $C_{l,max}$.

It has been shown that grit roughness applied to an otherwise clean airfoil can model the aerodynamic performance degradation due to ice roughness reasonably well. Busch[34] constructed a simulation based on glaze ice roughness accreted on a sub-scale, 18-inch chord NACA 23012 icing tunnel model. Based on measurements of a casting of the accretion, the average roughness height was k/c = 0.0025 on the upper surface of the airfoil and k/c = 0.0012 on the lower surface. Silicon carbide roughness elements of height k/c = 0.0026 were applied to an 18-inch chord NACA 23012 aerodynamic tunnel model at the appropriate chordwise extents to represent the ice roughness. The effects of the simulated roughness on C_l, C_m, and C_d were measured and compared with the effects of the casting. These data are shown in Fig. 11. General agreement was good between the casting and simulation for the

range of α over which the lift curve slope is linear. $C_{l,max}$ of the simulation was within 4% of the casting $C_{l,max}$. However, stall occurred about 1 degree earlier for the ice simulation than for the casting, resulting in differences in both $C_{l,max}$ and C_m at α = 10 deg. Agreement in C_d between the simulation and casting is good at positive angles of attack, but below α = 0 deg., the simulation has much higher C_d than the casting. The higher C_d of the simulation was likely caused by a larger average roughness height on the lower surface of the simulation than on the casting. No simulation was constructed which had different roughness sizes on the upper and lower surface in that study, but later data acquired by Busch et al.[6] suggest that a smaller roughness size on the lower surface would have likely improved agreement in C_d at negative angles of attack without adversely affecting the agreement at positive angles. In spite of the disagreement in C_d at low angles of attack, the results at positive angles of attack suggest that simple-geometry simulations of the same scale of a casting can reproduce the casting aerodynamics relatively accurately at identical Reynolds and Mach numbers if appropriate grit roughness is used.

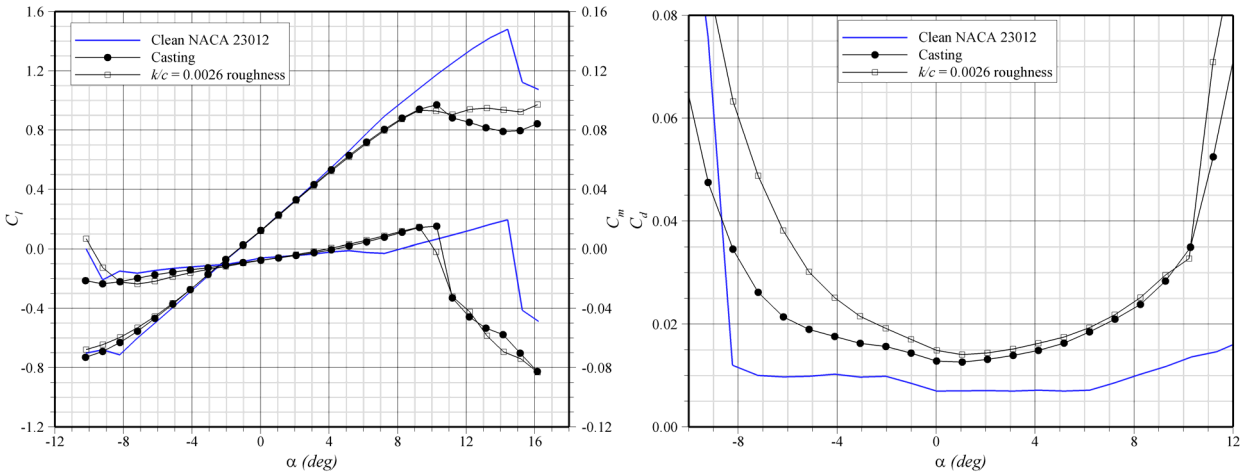

Fig. 11 Comparison between ice roughness casting and simulated ice roughness on an 18-inch NACA 23012 airfoil. Re = 1.8 x 10^6, M = 0.18[34]

Sub-scale simulation with full-scale validation

Busch et al.[6] simulated a full-scale ice roughness accretion using similar techniques. The accretion simulated consisted of glaze ice, or clear ice, a type of ice which forms at temperatures just below freezing. An artificial ice shape was constructed for an 18-inch chord NACA 23012 airfoil which had similar non-dimensional roughness height *k/c*, concentration, and chordwise extent as a casting of ice accreted on a 72-inch chord NACA 23012 airfoil. The height of the roughness on the simulation varied from *k/c*= 0.0003 – 0.0013 to match the variation in roughness height measured on the casting. Roughness concentration was also varied along the chord of the casting to better reproduce the casting surface roughness. A comparison of the aerodynamic performance between the simulation and casting is shown in Fig. 12. $C_{l,max}$ of the simulation is 4% lower and occurs about 1 degree earlier than for the casting, corresponding to an earlier break in C_m. This comparison is similar to that of Fig. 11. Also, C_d of the simulation below α = 4 deg. tended to be 20% - 30% higher than C_d of the casting at the same angle of attack. This simulation, unlike the simulation of Fig. 11, had roughness of the same *k/c* of the casting on the lower surface. Thus, at relatively low Reynolds number, the sub-scale simple-geometry roughness simulation tended to give a similar but slightly conservative estimate of the "true" iced-airfoil aerodynamic performance.

Busch et al.[6] also constructed a simulation of a second ice roughness accretion consisting of rime ice which had a smaller maximum roughness height and greater chordwise extents. Rime ice occurs at much lower temperatures than glaze ice and forms when water droplets freeze immediately upon impacting the airfoil (or ice accretion) surface. The casting had roughness extending from *x/c* = -0.002 – 0.080 on the upper surface and from 0.000 – 0.200 on the lower surface with a maximum height of *k/c* = 0.0003 on each surface. This simulation used grit roughness of height *k/c* = 0.0003, much smaller than that used on the glaze ice roughness simulation. The extents of the simulation roughness were from the airfoil leading edge to *x/c* = 0.03 on the upper surface and to *x/c* = 0.04 on the lower surface, shorter than the extents of the casting. Comparisons between the rime ice roughness simulation and the casting (Fig. 12) show that the simulation imparted a much larger degradation in $C_{l,max}$ than did the casting. This difference in $C_{l,max}$ may have in part been due to a higher concentration of roughness on the simulation than on the casting. At the time of testing, it was thought that the roughness concentration on the casting was above the

critical concentration, based on Fig. 10. Therefore, with the expectation that changes in roughness concentration would have only minimal impact on $C_{l,max}$, a high roughness concentration was used on the simulation to ensure uniformity of distribution and repeatability. Because the casting roughness was so small, it is possible that the roughness concentration was not above the critical concentration, resulting in a larger decrease in $C_{l,max}$ of the simulation. C_d at low angle of attack was also larger for the simulation than for the casting, but agreed well with the casting at higher angles of attack prior to stall. This trend in C_d is consistent with the simulations of both the full-scale and sub-scale glaze ice roughness castings discussed earlier.

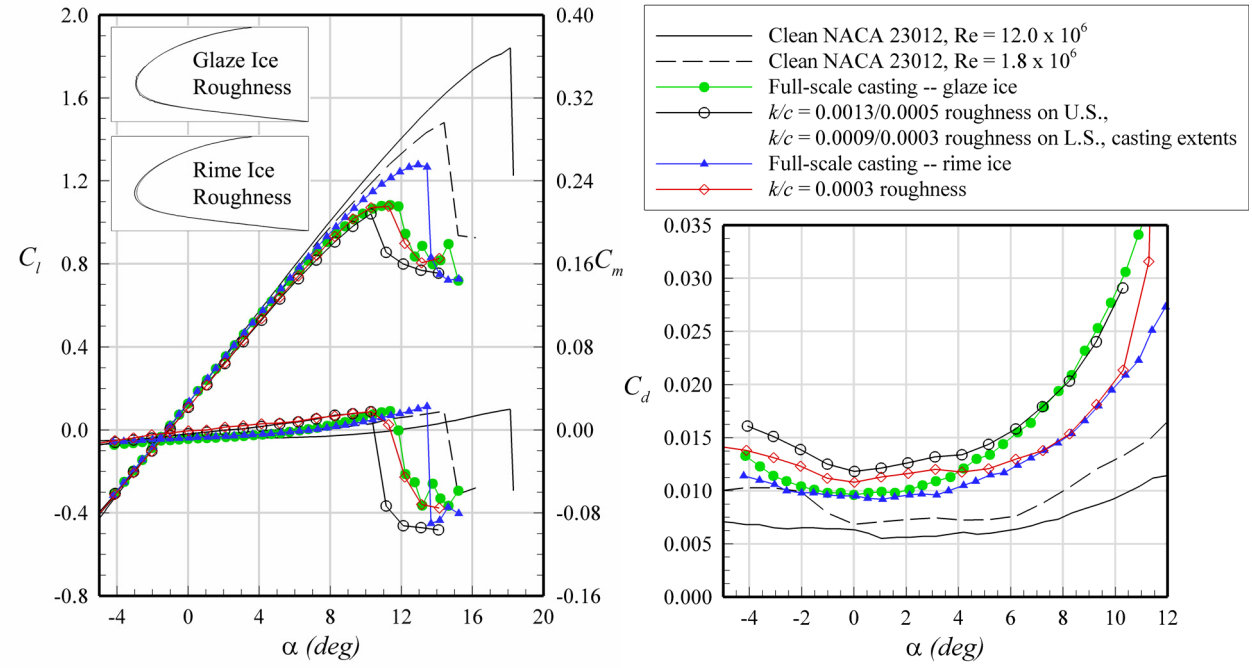

Fig. 12 Comparison between full-scale glaze and rime ice roughness castings and sub-scale simulated ice roughness on a NACA 23012 airfoil. Full-scale data acquired at Re = 12.0 x 10^6 and M = 0.18, sub-scale data acquired at Re = 1.8 x 10^6, M = 0.18.[6]

Streamwise Ice

A streamwise-ice accretion differs from ice roughness in that there often exists a large leading-edge ice geometry. The geometry may introduce a strong adverse pressure-gradient, causing a short separation bubble to form. This bubble does not usually have a global impact on the pressure distribution around the airfoil, and much of the performance degradation due to streamwise ice is through the effects of surface roughness. These effects are similar to those caused by ice roughness, coming mainly from the interaction between the roughness elements and the developing boundary layer and causing premature trailing-edge separation.

Important geometric features

Busch[34] conducted a study which examined the effects of roughness height and concentration on 2-D smooth and simple-geometry streamwise-ice simulations. As with ice roughness, $C_{l,max}$ tended to decrease as roughness height increased (Fig. 13(a)). To determine the effect of roughness concentration on $C_{l,max}$, two different roughness heights, k/c = 0.0009 and k/c = 0.0026, were applied to a 2-D smooth simulation. For very low concentrations, increasing the concentration caused $C_{l,max}$ to decrease (Fig. 13(b)). At some critical concentration, $C_{l,max}$ became much less affected by further increases. This trend is very similar to that observed for ice roughness, suggesting that surface roughness alters the boundary layer development in a similar way for ice roughness and streamwise ice accretions. This result is not surprising, as conformal streamwise-ice accretions frequently act as leading-edge extensions.[35]

Another consideration for designing streamwise-ice simulations is that the exact shape and size of the gross leading-edge geometry does not usually have a large impact on the iced-airfoil $C_{l,max}$. For example, Kim and Bragg[36] showed that, for a simple-geometry simulation of a streamwise-ice accretion on a NLF-0414 airfoil,

moderate changes in the height of the accretion did not have a large effect on $C_{l,max}$. This in contrast to a horn-ice accretion, where it has been shown that small changes in horn height do have a large effect on $C_{l,max}$.[19] Though the effect of streamwise-ice height on $C_{l,max}$ is small, Kim and Bragg found that its effect on C_m is significant. In another study, Busch et al.[6] constructed two types of streamwise-ice simulation on a NACA 23012 airfoil, a simple-geometry and 2-D smooth simulation, which had slightly different leading-edge geometries. For a given level of surface roughness, different leading-edge geometries had only a small effect on iced-airfoil aerodynamic performance (Fig. 14). It is clear that the presence of a geometry on the leading edge that alters the airfoil profile is important to represent, although these results indicate that its shape is not critical.

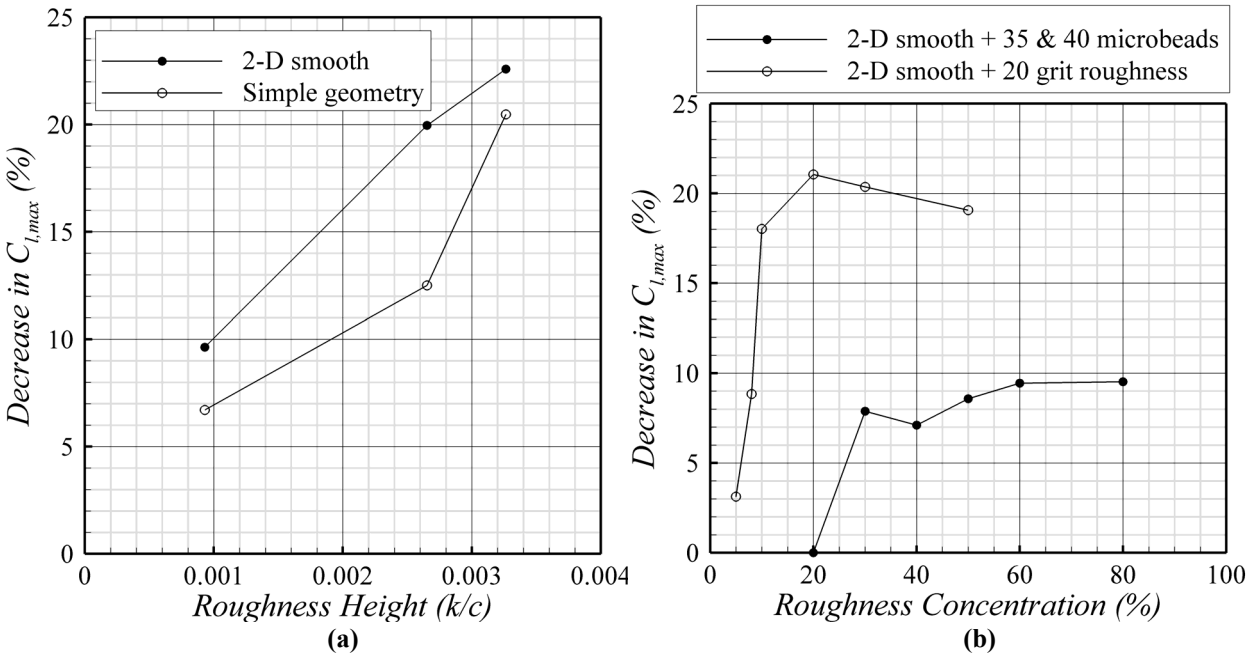

Fig. 13 (a) Effect of surface roughness height on $C_{l,max}$ of 2-D smooth and simple-geometry streamwise-ice simulations, and (b) effect of roughness concentration on $C_{l,max}$ of a 2-D smooth streamwise-ice simulation.[34]

Highly three-dimensional ice feathers or nodules are often present on streamwise ice accretions (Fig. 15(a)). Feathers are usually larger than ice roughness and can not be characterized fully using ice tracings. Because most ice simulations are two-dimensional, they can not usually reproduce the aerodynamic effects of ice feathers. To help overcome this shortcoming, feathers are usually considered to be a form of surface roughness and grit roughness is applied to two-dimensional simulations to better represent them. However, since feathers are much larger than ice roughness, they may impact the tracing of the ice accretion used to construct the 2-D simulation, which is meant to capture only the gross ice geometry. An example depicting this is shown in Fig. 15(b), where feathers that were traced on the upper and lower surface have been circled. The tracing of these feathers introduced artificial "ridges" in the 2-D smooth simulation. Busch et al.[6], while developing sub-scale methods for simulating ice accretion, measured the effects of these traced feathers by comparing C_l, C_m, and C_d of the 2-D smooth simulation with the extruded feathers and one in which the feathers were faired. The results are presented in Fig. 14, in which the 2-D smooth simulation with no roughness has faired feathers. These plots show that the effect of the two-dimensionalized feathers was to reduce $C_{l,max}$ by 0.06 and increase $C_{d,min}$ by 0.0013. It is evident that the artificial ridges introduced by the extrusion of these feathers caused a more severe performance degradation than did the true geometry of the ice feathers present on the casting. This example illustrates that a tracing must be appropriately interpreted to determine whether it represents the true accretion geometry.

Sub-scale simulation with full-scale validation

Also shown in Fig. 14 is a 2-D smooth simulation with roughness added. This simulation was constructed by Busch et al.[6] to reproduce the aerodynamics of a full-scale streamwise-ice casting at Re = 12.0 x 10^6 and M = 0.20. The roughness had similar non-dimensional height and extent as roughness on the casting, but it is evident from Fig. 14 that this caused too large an aerodynamic penalty, resulting in α_{stall} and $C_{l,max}$ lower than the casting and C_d higher

than the casting at all angles of attack. It appears from Fig. 14 that a more accurate simulation was the 2-D smooth simulation with no roughness. The simple-geometry simulation with no roughness and 2-D smooth simulation (with small ridges, as explained earlier) also had $C_{l,max}$ and C_d closer to the casting than did the 2-D smooth simulation with roughness.

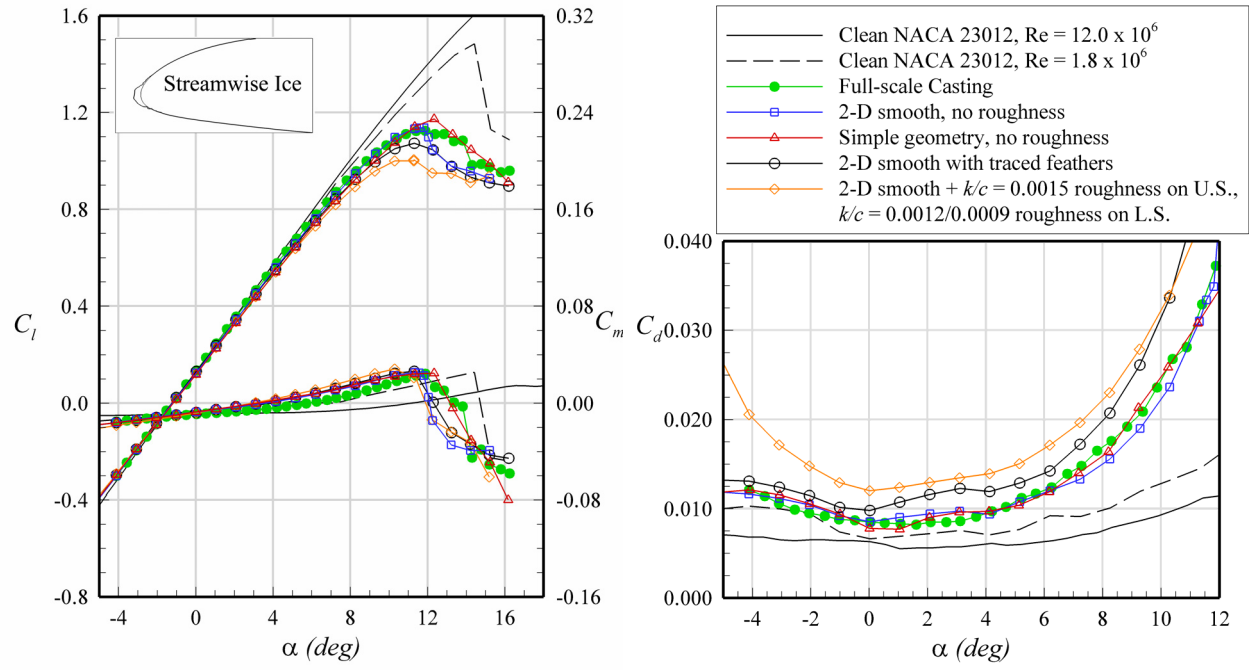

Fig. 14 Comparison of C_l, C_m, and C_d of various 2-D smooth and simple-geometry streamwise-ice simulations with a streamwise-ice casting. The casting data were acquired at Re = 12.0 x 10^6 and M = 0.20, and the simulation data were acquired at Re = 1.8 x 10^6 and M = 0.18.[6]

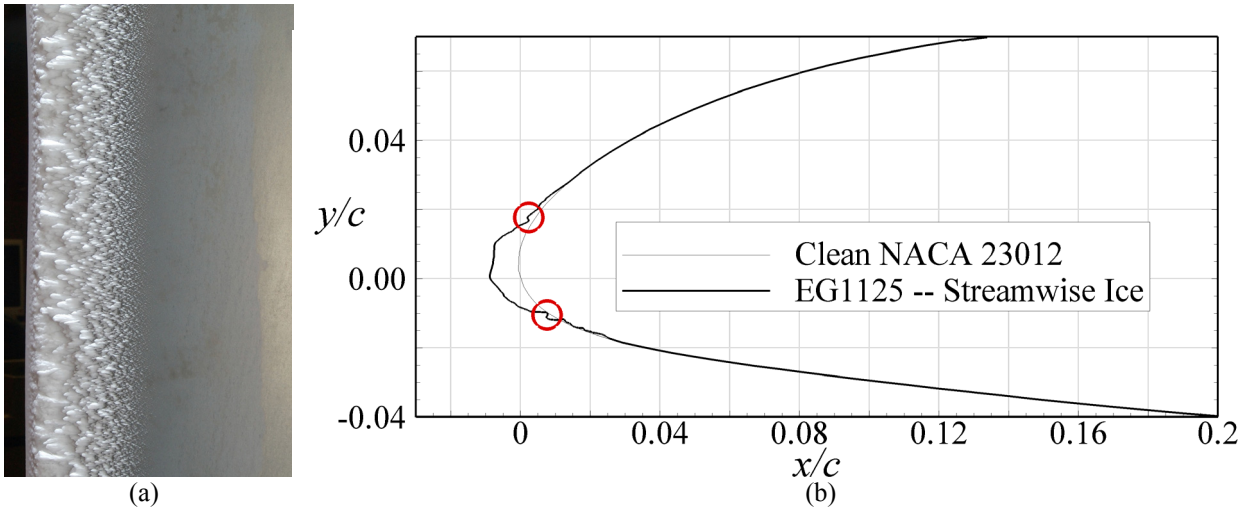

Fig. 15 (a) Photograph of ice feathers on a streamwise-ice accretion located near the leading-edge on the upper surface of a NACA 23012 airfoil and (b) a tracing of the same streamwise-ice accretion with traced feathers circled.[6]

Current sub-scale simulation techniques were again applied to determine the accuracy with which a second full-scale casting of a streamwise ice accretion, also tested by Broeren et al.[5] at Re = 12.0 x 10^6 and M = 0.20, could be modeled. Comparisons of aerodynamic performance between the full-scale casting and sub-scale simulations are

shown in Fig. 16. Both the 2-D smooth and simple-geometry simulations had a higher $C_{l,max}$ than the casting. This is also evident in the comparison of the C_d curves, as both simulations had lower C_d at positive angles of attack. The 2-D smooth simulation likely imparted a slightly worse aerodynamic penalty than did the simple-geometry simulation because it had a small amount of two-dimensionalized surface roughness due to tracing of roughness elements present on the casting. When surface roughness of the same k/c and extents of the casting was added to the 2-D smooth simulation in an effort to better model the performance of the casting, it caused too low of a $C_{l,max}$ and too high of a C_d. This was consistent with the ice roughness simulations and the other streamwise-ice accretion. As discussed earlier, this may in part be due to Reynolds number effects and should be explored further. From these studies, however, it appears as if the full-scale casting aerodynamic performance can be bracketed by sub-scale 2-D smooth streamwise-ice simulations with and without roughness.

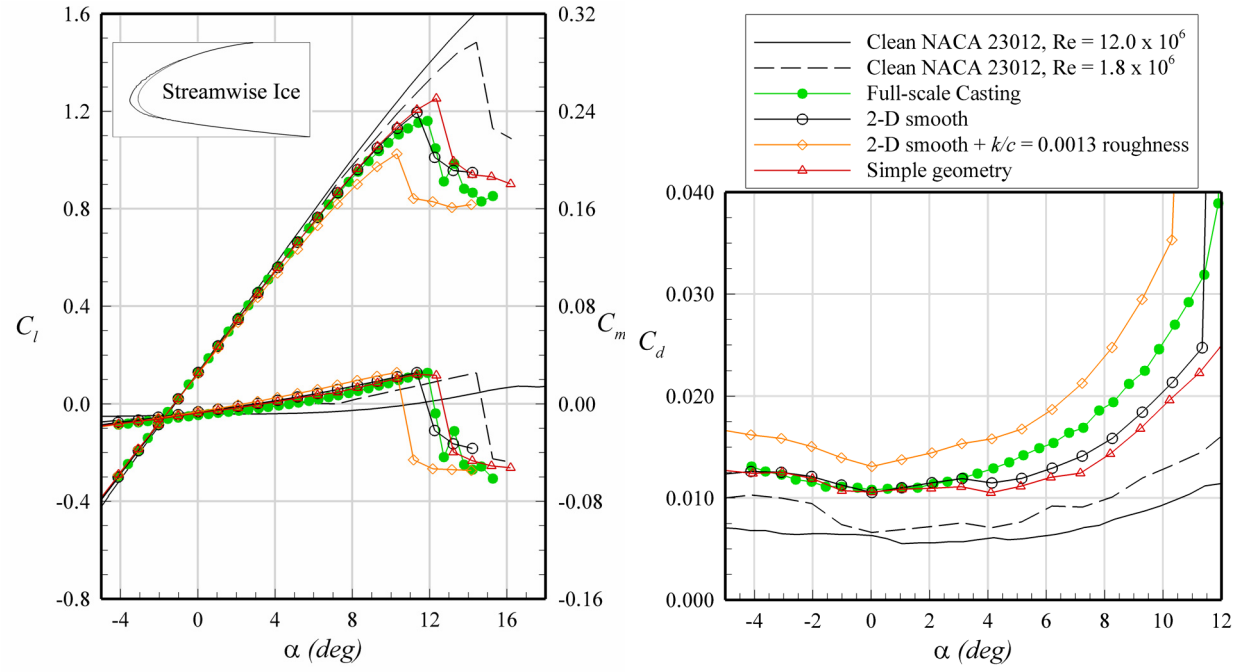

Fig. 16 Comparison of C_l, C_m, and C_d of various 2-D smooth streamwise-ice simulations with a streamwise-ice casting. The casting data were acquired at Re = 12.0 x 10^6 and M = 0.20, and the simulation data were acquired at Re = 1.8 x 10^6 and M = 0.18.[6]

Horn Ice

Previous research on horn-ice accretions has shown that the iced-airfoil flowfield is dominated by a long separation bubble generated by an adverse pressure gradient at the tip of the horn. The size of the separation bubble for given flow conditions is determined by the pressure gradient in which it occurs (a function of chordwise location and airfoil geometry) and gross horn geometry, which can be characterized by the horn height, angle with respect to the chord line, and sometimes horn tip radius. Surface roughness has been shown to have relatively smaller effects on iced-airfoil performance. This section covers the effects of changes in the gross horn geometry and which features need to be appropriately represented on sub-scale simulations. Bragg et al.,[3] Jacobs,[37,38] and Gurbacki[16,39] discuss the horn-ice flowfield in more detail.

Important geometric features

Busch et al.[1,26] investigated the level of detail required to accurately represent a horn-ice casting using simulations of varying fidelity. The iced-airfoil performance measured for each of these simulations was compared to that measured for the casting on an 18-inch chord NACA 23012 airfoil. Both 3-D simulations and 2-D simulations were constructed to determine the importance of representing spanwise variation in the horn geometry. The 3-D simulations were based on measurements of the casting and varied horn height and angle along the span to match the spanwise variation present on the casting. One of the 2-D simulations was a 2-D smooth simulation, which captured

the detailed ice geometry at only a single spanwise station, and the other was a simple-geometry "spoiler" type simulation in that a rectangle was used to model only horn height and angle. This study showed that the 2-D smooth and simple-geometry simulations were able to reproduce aerodynamic performance nearly as well as the more sophisticated simulations and that it is not necessary to add surface roughness to achieve good agreement.

While the 2-D simulations were able to reproduce the aerodynamic performance of the casting with reasonably good accuracy, they were not able to reproduce the surface flowfield. Gurbacki,[39] Blumenthal, and Busch et al.[26] used fluorescent oil-flow visualization, a technique which relies on surface shear stresses to show flow direction and time-averaged flowfield features such as mean separation bubble reattachment and transition, to compare the flowfields of castings and 2-D smooth simulations (Fig. 17). In the image, flow is from left to right, and the 3-D casting is visible on the left of Fig. 17(a). The horizontal scales at the top and bottom of the picture correspond to the chordwise station in percent chord, while the vertical scale on the right measures the spanwise station in inches. The speckled region in the figure indicates the mean reattachment zone of the separation bubble, which ranges from x/c = 0.25 near the top of the model to x/c = 0.28 near the bottom of the model. Inside of the separation bubble is a region of reverse flow, indicated by the oil streaks flowing from right to left. Note that the separation bubble of the casting contains highly three-dimensional cell structures. In contrast, the flowfield behind the 2-D smooth simulation is almost completely two-dimensional (Fig. 17(b)). Jacobs[37] showed that the cellular structures in the flowfield of a 2-D smooth simulation with roughness were formed by discrete, quasi-steady streamwise vortices non-uniformly distributed across the airfoil span. Streamwise vortices were also present behind a 2-D smooth simulation without roughness, but the distribution was much more uniform, resulting in the more two-dimensional flowfield. In studies by Jacobs[37] and Gurbacki,[16] these cell structures were generated on 2-D smooth simulations by adding grit roughness to the horn, but in another study by Busch,[34] the horn-ice flowfield remained two-dimensional even after the addition of grit roughness. However, streamwise vorticity does not appear to have a substantial effect on $C_{l,max}$ and is therefore not necessary to exactly represent for most simulation needs.

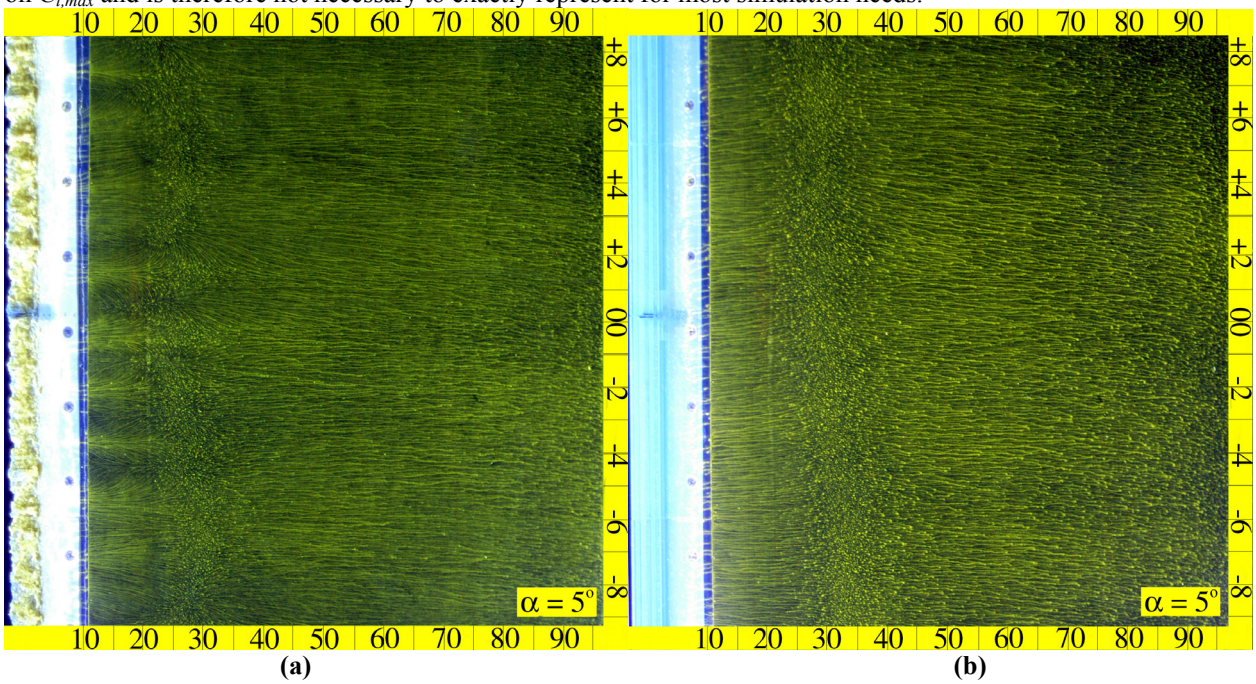

Fig. 17 Comparison of the surface flowfield behind a (a) horn-ice accretion casting and a (b) 2-D smooth horn-ice simulation. The mean separation bubble reattachment line has been highlighted. Re = 1.8x10^6 and M = 0.18.[26]

Since the iced-airfoil flowfield does not depend strongly on the detailed horn geometry, horn-ice can be represented using simple-geometry simulations, which makes it easy to conduct parametric studies to determine the effects of parameters such as horn height, angle, and location. The effects of these parameters have been investigated in the past by Kim[36] and Papadakis et al.[40] In the former study, simple-geometry simulations of various heights were installed on a NLF-0414 airfoil model at several chordwise locations, and in the latter, spoiler-ice simulations of two different heights were installed at two chordwise locations and several different angles on a NACA 0011 airfoil. Both studies found $C_{l,max}$ to decrease as horn height increased for a given positive surface

location and horn angle, and Kim showed that $C_{l,max}$ decreased more rapidly with increasing height for farther aft locations to $s/c = 0.034$. In looking at the effects of horn location, Kim observed $C_{l,max}$ to decrease almost linearly as the horn location s/c increased from -0.012 to 0.034 for a constant horn height, with larger horn heights causing $C_{l,max}$ to decrease more rapidly. Papadakis et al. also found $C_{l,max}$ to decrease with increasing s/c. In addition, Papadakis et al. reported that for a given horn height ($k/c = 0.0625$) and location ($x/c = 0.02$), the degradation in $C_{l,max}$ increased as θ increased from 10 to 90 deg., but then decreased as θ increased further to 130 deg.

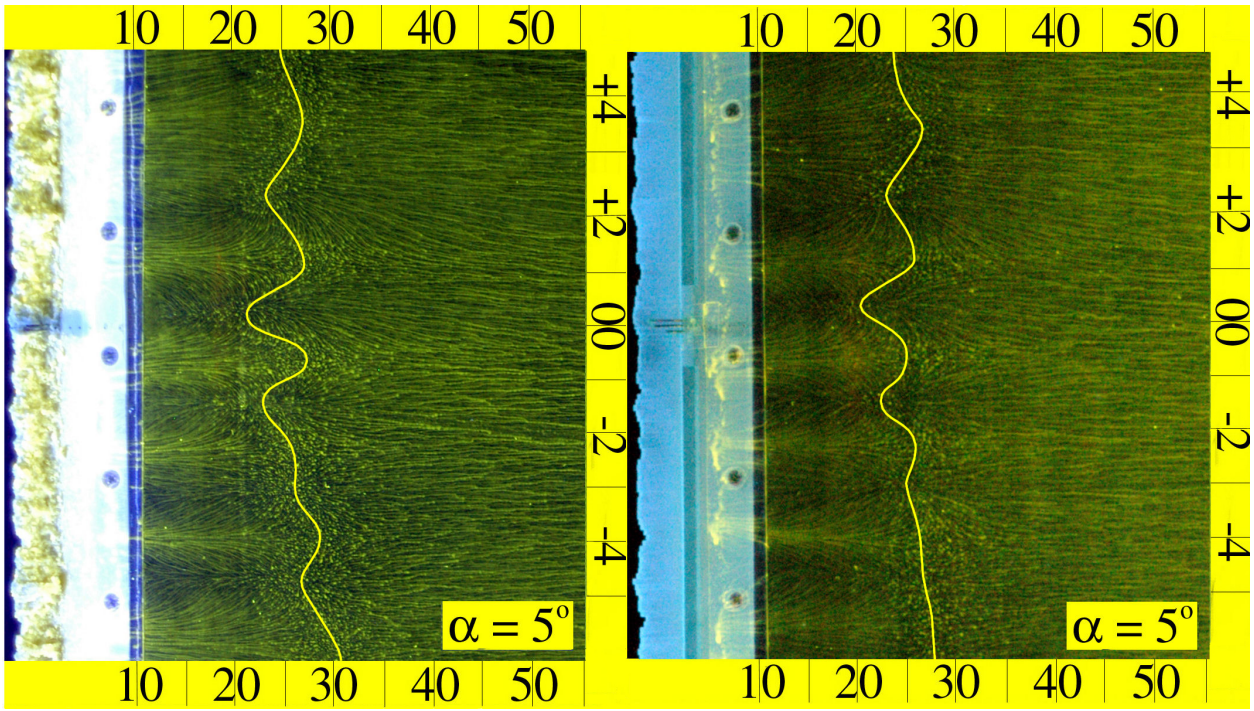

Fig. 18 Comparison of the surface flowfield behind an (a) ice accretion casting and a (b) simple-geometry simulation with spanwise variation. This image is of the center third of the airfoil model only. The mean separation bubble reattachment line has been highlighted. Re = 1.8x10^6 and M = 0.18. [26]

The degradation in $C_{l,max}$ measured in several studies for various horn heights and airfoil geometries are compared in Fig. 19 for horns located near $s/c = 0.01$ and 0.02. For each study in which multiple data points are available, such as that of Broeren et al.[41] which looked at the effects of simulated horn-ice on three different airfoil geometries, the degradation in $C_{l,max}$ is seen to increase slightly with increasing horn height. The plot shows that some airfoil geometries, such as the NACA 0012 and 23012, tend to be more sensitive to horn-ice of a given height for a given location. The NLF-0414 and NACA 3415 airfoils have very similar sensitivities to horn-ice for horns located near $s/c = 0.017$, as horns with the same heights and locations caused nearly identical reductions in $C_{l,max}$ on these two airfoils. The sensitivity of $C_{l,max}$ to horn height k/c shown in Fig. 19 is highly dependent on surface location s/c and may differ for horns at different locations.

Kim and Bragg[42] examined the effect of horn tip radius on $C_{l,max}$ and C_d of a NLF-0414 using simple-geometry simulations and found that for a horn of height $k/c = 0.022$ it had little impact. In contrast, Blumenthal et al.[19] found that decreasing the horn tip radius on a 2-D smooth horn-ice simulation for a similarly sized and located horn ($k/c = 0.027$, $s/c = 0.020$) on a NACA 0012 airfoil reduced $C_{l,max}$ by about 8% and increased C_d at all positive angles of attack. This discrepancy is likely due in part to the increased sensitivity of the NACA 0012 to ice contamination relative to the NLF-0414. For larger horns which caused larger performance penalties on the NLF-0414, Kim[36] recorded increasing sensitivity to horn tip radius as the horn height increased or the location moved toward the trailing edge of the airfoil. Tip radius had the largest effect on the largest, farthest aft horn ($k/c = 0.067$, $s/c = 0.034$), where decreasing horn tip radius reduced $C_{l,max}$ by 22%. Most horns, however, are smaller and located farther upstream where the sensitivity to tip radius is somewhat less.

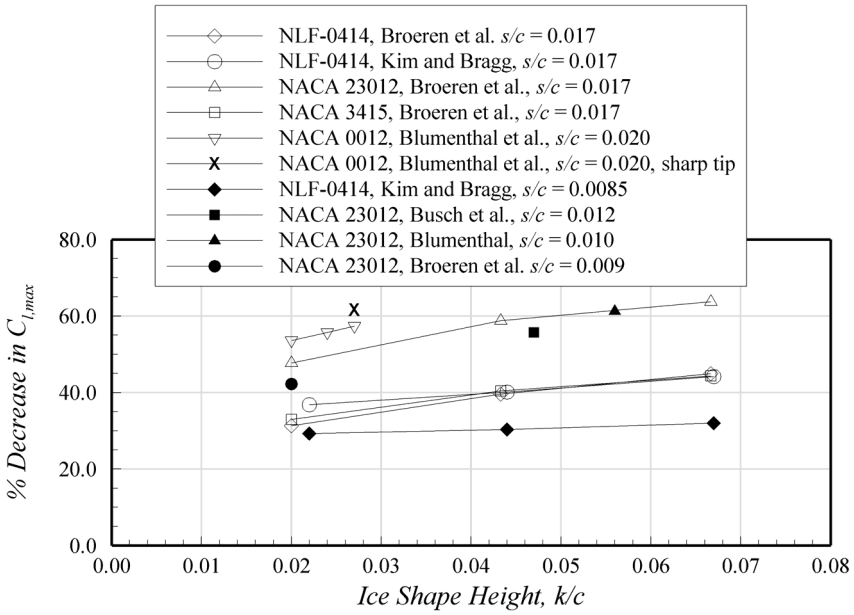

Fig. 19 Effect of horn height on iced-airfoil $C_{l,max}$ for various airfoils. Data from Broeren et al.,[41] Kim and Bragg,[42] Blumenthal et al.,[19] Busch et al.,[1] Blumenthal,[25] and Broeren et al.[5]

Frequently horn-ice accretions have lower surface horns in addition to upper-surface horns. Kim and Bragg[42] and Blumenthal et al.[19] have shown that the presence of a lower surface horn on 2-D smooth and simple-geometry simulations has little effect on iced-airfoil aerodynamics at high angles of attack near $C_{l,max}$. At low lift coefficients, lower-surface horns tend to increase drag (Fig. 20), and they may also affect the negative stall angle of attack and decrease the magnitude of negative $C_{l,max}$. Bragg et al.[3] and Kim[36] discuss that the total drag on the iced airfoil with upper and lower horns can be approximated as the linear combination of the drag increments of the upper and lower surface horns:

$$C_{d,total} = C_{d,clean} + (C_{d,upper} - C_{d,clean}) + (C_{d,lower} - C_{d,clean}) \tag{3}$$

This is illustrated in Fig. 20. The line marked "sum" in the figure uses the formula above to estimate the drag polar of the airfoil with both upper and lower surface horns, and the curve is remarkably similar to the measured drag polar at all angles of attack shown. For simulation of ice accretion at angles of attack of a practical interest, the effect of the lower surface horn is mainly to increase C_d at low angle of attack, and this effect diminishes with increasing angle of attack. This phenomenon has been observed for other types of ice accretion as well, such as spanwise-ridge ice.[9]

To isolate the effects of surface roughness, many studies have compared identical 2-D simulations of horn-ice with and without roughness and documented its effect. In these studies the presence of surface roughness had differing effects. Busch[34] found that $k/c = 0.0037$ roughness caused $C_{l,max}$ to decrease and C_d to increase on a NACA 23012. Jacobs and Bragg[38] observed separation bubble size to decrease with the addition of $k/c = 0.0059$ roughness to a NACA 0012 horn-ice simulation. No performance data were reported in that study, but a decrease in separation bubble size usually corresponds to an increase in $C_{l,max}$ and a decrease in C_d. Blumenthal et al.[19] added $k/c = 0.0037$ roughness to the front face of a horn on a NACA 0012 and found $C_{l,max}$ to decrease and C_d to increase at low angles of attack. Papadakis et al.[43] observed only very small reductions in $C_{l,max}$ with the addition of $k/c = 0.00058$ roughness to a horn on a modified NACA 63_A-213 airfoil. Addy et al.[18] found that the addition of $k/c = 0.00078$ roughness to horn ice on a GLC-305 airfoil had no effect on the airfoil $C_{l\,max}$ and only a minor effect on C_d. The authors in this study proposed that various methods of applying grit roughness may yield differing results, as there are no standardized methods for determining appropriate roughness sizes or concentrations. Indeed, the non-dimensional roughness heights used in these studies varied greatly, with roughness of height less than $k/c = 0.00078$ having only a small effect on iced-airfoil performance and roughness of height $k/c = 0.0058$ improving performance. Roughness heights in the range between these heights tended to degrade performance. It is likely that the sensitivity of the airfoil to ice accretion is also important, as each of these studies were conducted on different airfoils.

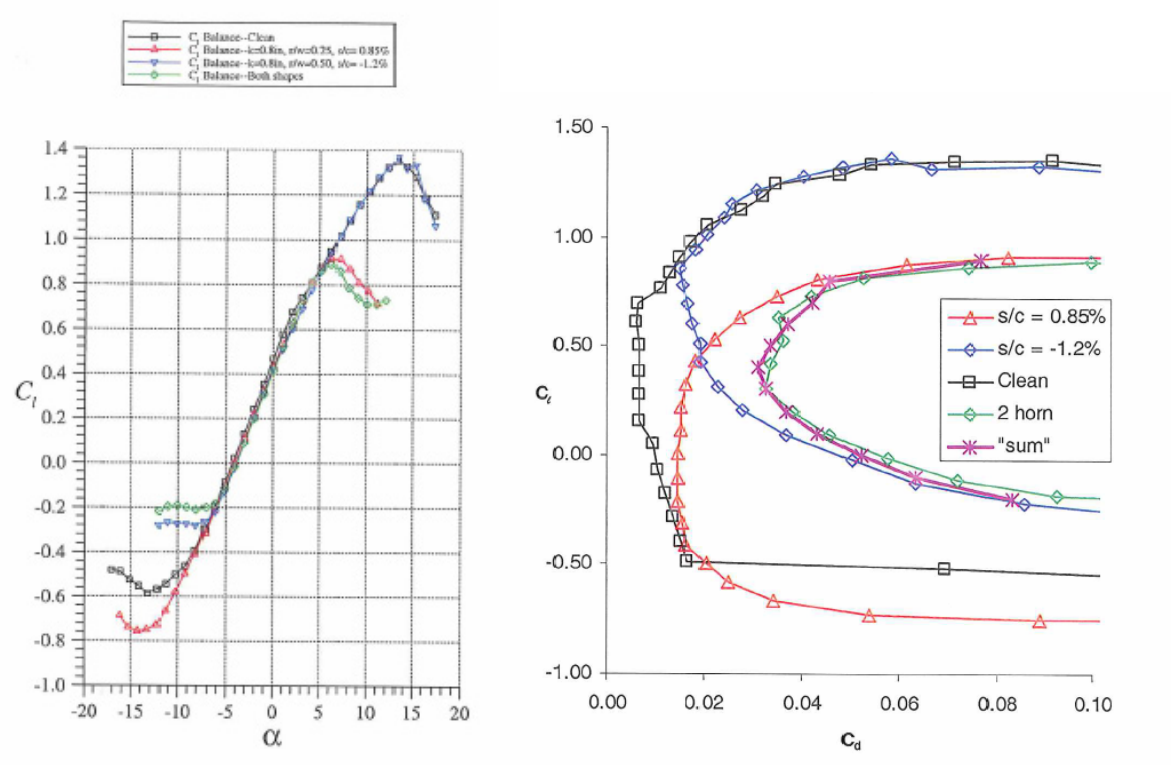

Fig. 20 Effect of upper and lower surface horns on NLF-0414 airfoil C_l and C_d at Re = 1.8 x 10^6 and M = 0.18.[36]

In regards to improving simulation aerodynamic fidelity for horn-ice accretions, surface roughness has not been shown to be universally effective, and if not applied appropriately, may worsen simulation fidelity. Busch[34] compared the aerodynamic performance of a 2-D smooth simulation of a horn-ice accretion with and without surface roughness to its corresponding casting. The aerodynamic performance of the 2-D smooth simulation without roughness was found to better reproduce the performance of the casting, as adding surface roughness resulted in estimates of $C_{l,max}$ and C_d which were too conservative.

Sub-scale simulation with full-scale validation

The above considerations regarding horn-ice simulation design were employed by Busch et al.[6] in constructing sub-scale 2-D simulations of a full-scale horn-ice accretion casting. The aerodynamic performance of a 72-inch chord NACA 23012 airfoil with a horn-ice casting is discussed in detail by Broeren et al.[5] at Reynolds numbers from 4.6 x 10^6 – 16.0 x 10^6 and M = 0.10 - 0.28, and is considered to be representative of the true iced-airfoil aerodynamics. Both 2-D smooth and simple-geometry simulations were constructed at ¼-scale and tested at Re = 1.8 x 10^6 and M = 0.18 by Busch et al. Comparisons between this sub-scale data and the full-scale data at Re = 12.0 x 10^6 and M = 0.20 are shown in Fig. 21. The 2-D smooth simulation had C_l and C_d very similar to the casting at most angles of attack, while the simple-geometry simulation had $C_{l,max}$ too low and C_d too high. The authors suggest that this discrepancy was due to positioning inaccuracies and poor tolerances in the simple-geometry simulation, as it was constructed from off-the-shelf materials rather than fabricated from rapid-prototyping techniques (as was the 2-D smooth simulation). However, the simple-geometry simulation was intended to provide an indicator of how accurate a low cost, easy-to-produce simulation could represent the true iced-airfoil aerodynamics. Note that the uncertainty in ice accretion geometry due to the effects of tracing location and icing tunnel repeatability (Fig. 2 - Fig. 6) results in uncertainties in aerodynamic performance which may be on the order of the differences seen with the horn-ice simulations of Fig. 21.

Spanwise-ridge Ice

As discussed in the Introduction, spanwise-ridge ice often forms behind a thermal ice protection system operating at less than 100% evaporation, most frequently in super-cooled large droplet (SLD) conditions due to accretion behind an ice protection system. The airfoil leading edge generally is clean and free of ice, and the boundary layer has time

to establish before reaching the accretion. Spanwise ridges frequently generate separation bubbles. Broeren et al.[9] have classified two types of spanwise-ridge accretion: short ridges, which generate short separation bubbles, and tall ridges, which generate long separation bubbles. The two types of ridges require different techniques to properly simulate, since geometric features that are important on short ridges are not necessarily important on tall ridges, and vice versa. This section discusses important geometries features on each type of ridge and current methods for simulating spanwise-ridge ice accretions.

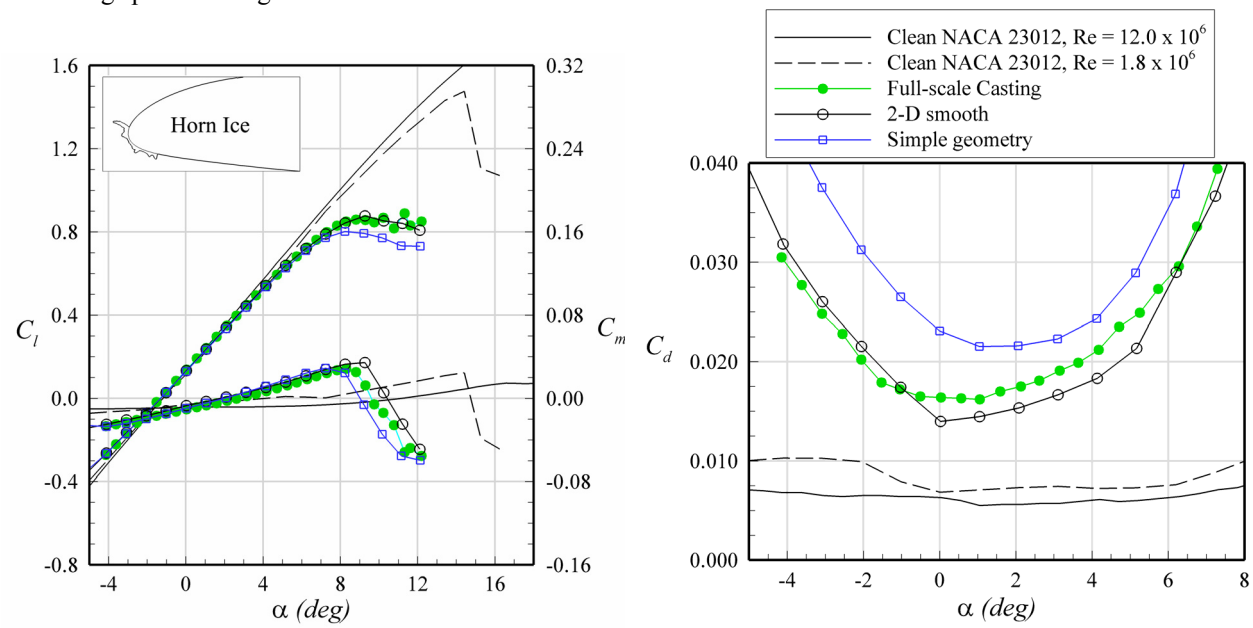

Fig. 21 Comparison of aerodynamic performance of sub-scale horn-ice simulations at Re = 1.8 x 10^6 and M = 0.18 with the corresponding full-scale casting at Re = 12.0 x 10^6 and M = 0.20.[6]

Tall Ridges

Tall ridges are usually much greater than the local boundary-layer height and generate long separation bubbles, similar to horn-ice accretions. As with horn ice, the flowfield is dominated by the separation bubble and larger bubble sizes tend to correspond with larger performance degradations. Recall that the long separation bubble increases in size with increasing angle of attack and has a global effect on the flowfield. The effect of a tall ridge on the pressure distribution of a NACA 23012 airfoil is shown in Fig. 22. In the figure, a tall ridge is located at x/c = 0.05 on the upper surface of the airfoil (the lower surface ridge is located at x/c = 0.10). The ridge prevents the formation of the suction peak which normally forms near the leading edge on the clean airfoil. With the ridge, the C_p in this region remains positive. There is a rapid increase in pressure as the flow decelerates immediately in front of the ridge followed by a sharp decrease in pressure at x/c = 0.05 as the flow accelerates over the top of the ridge. Downstream of this extreme decrease in pressure is a region of constant pressure, indicative of a separation bubble. Near x/c = 0.20, pressure recovery begins, but the iced C_p distribution never matches that of the clean airfoil, as the trailing-edge pressure is lower in the iced case. Thus, the tall ridge has a global effect on the airfoil pressure distribution, altering it from leading-edge to trailing edge. Broeren et al.[9] discuss in additional detail the flowfields of tall ridge ice accretions.

Important geometric features

To determine the sensitivity of iced-airfoil performance to variations in ridge geometry, Lee[44] performed a study analogous to Kim's study of horn-ice geometry.[36] Quarter-round simple-geometry simulations of ridge ice of various heights were placed at various locations on a NLF-0414 and modified NACA 23012 airfoil, both with 18-inch chords. As with horn-ice accretions located at positive s/c (i.e., on the upper surface of the airfoil), the degradation in airfoil $C_{l,max}$ and C_d increased with increasing ridge height. This is shown for the $C_{l,max}$ of the NACA 23012m airfoil in Fig. 23. Whalen et al.[14] also found $C_{l,max}$ to decrease with increasing ridge height.

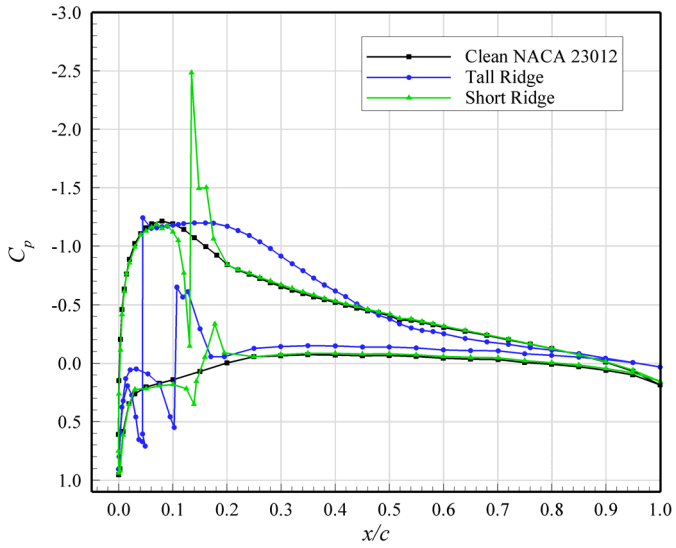

Fig. 22 Effect of tall and short ridges on pressure distribution of NACA 23012 airfoil at Re = 12.0 x 10^6 and M = 0.20.

Also shown in Fig. 23 is the dependence of $C_{l,max}$ on ridge surface location for a modified NACA 23012 airfoil. Ridges located at x/c = 0.10 to x/c = 0.12 caused the largest changes in $C_{l,max}$ and in C_m. Lee and Bragg[45] explain that ridges in this region were located just upstream of the maximum adverse pressure gradient on the NACA 23012 airfoil. The large adverse pressure gradient in which the separation bubble formed made it especially difficult for the separated shear layer to entrain sufficient high energy flow to reattach. This resulted in larger separation bubbles and correspondingly large aerodynamic penalties. Lee[44] shows that on a NLF-0414 airfoil, which has only a very slight adverse pressure gradient over much of its chord, $C_{l,max}$ is relatively insensitive to ridge location. Lee et al.[46] note that the ridge location at which C_d was most affected did not exactly correspond with that at which $C_{l,max}$ was most affected. Instead, C_d was increased most by ridges located slightly farther upstream, near the region of maximum local air velocity ($C_{p,min}$).

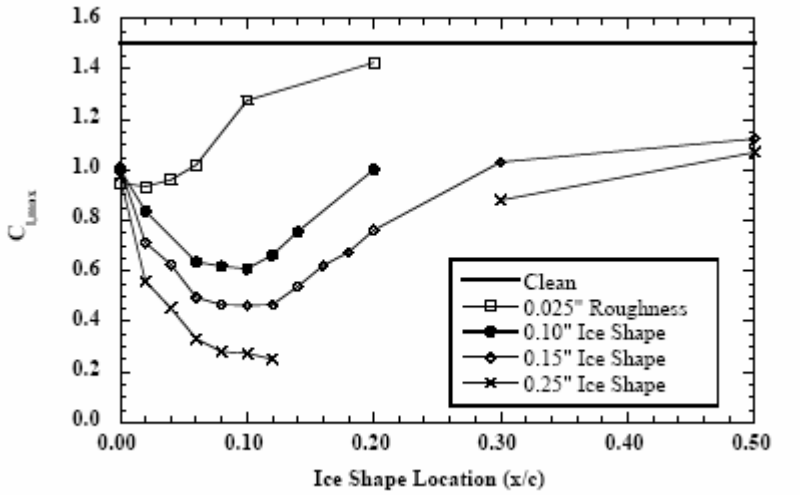

Fig. 23 Effect of simple-geometry ridge height and location on $C_{l,max}$ of a NACA 23012m airfoil.[44]

The 0.025" roughness in Fig. 23 corresponds to a strip of k/c = 0.0014 roughness with width s/c = 0.028 (with no ridge). Unlike the ridges, the roughness had the largest effect on $C_{l,max}$ when located near the leading edge. Lee[44] notes that this is because a ridge affects the airfoil performance through a different mechanism than the roughness. The ridge causes a separation bubble to form which grows with angle of attack, and $C_{l,max}$ occurs when

the airfoil is at sufficiently high angle of attack that the separation bubble does not reattach. This is a thin-airfoil type stall. In contrast, roughness causes early boundary-layer transition and extracts momentum. This eventually causes premature trailing-edge separation and ultimately results in trailing-edge stall. Lee reasoned that the momentum loss due to the roughness had the greatest effect when the roughness was located at the leading edge – this is consistent with the results of Brumby (Fig. 9). Lee also explains that each ridge, regardless of height, caused similar penalties to $C_{l,max}$ as the roughness when located at the airfoil leading edge. At this location, the ridges were in a favorable pressure gradient. The separation bubble remained small and stable, and the main effect of the ridge was to extract momentum and cause early boundary layer transition in a manner similar to the roughness. Note that these results are very similar to those observed by Kim and Bragg[42] for simple-geometry horn-ice simulations located near the airfoil leading edge.

In addition to using surface roughness alone, Lee and Bragg[47] also added surface roughness to some of the simple-geometry ridge simulations. It was found that, in general, roughness had a measurable effect on $C_{l,max}$ and C_d. This effect was dependent on the chordwise extent of the roughness. Roughness entirely within the separation bubble upstream or downstream of the ridge caused only a slight decrease in $C_{l,max.}$ Roughness extending far upstream of the upstream ridge separation bubble caused a slight increase in $C_{l,max}$. Lee[44] explained that this was likely due to the roughness displacing the boundary layer upwards, reducing the effective ridge height and decreasing separation bubble size. Busch et al.[6] added surface roughness on and downstream of the ridge on 2-D smooth and simple-geometry tall ridge simulations. A slight decrease in $C_{l,max}$ and increase in C_d was measured, consistent with the results of Lee. Whalen[15] measured the aerodynamic performance of NACA 3415 and 23012 airfoils with both 2-D and 3-D simple-geometry simulations. While this study was not conducted to determine the effect of surface roughness alone, the height, shape, and location of the upper surface ridge on the 2-D and 3-D simulations was similar. The trends in this study agreed with those observed by Lee and Busch et al.; $C_{l,max}$ was found to be consistently lower on the 3-D simulations, and C_d was higher at positive angles of attack on the 3-D simulations than on the 2-D simulations.

Sub-scale simulation with full-scale validation

Broeren et al.[5] obtained aerodynamic performance data on a casting of a tall spanwise ridge on a 72-inch chord NACA 23012 at Re = 12.0 x 10^6 and M = 0.20. Busch et al.[6] constructed sub-scale 2-D smooth and simple-geometry simulations of the casting and measured aerodynamic performance of an 18-inch chord NACA 23012 with the simulations installed at Re = 1.8 x 10^6 and M = 0.18. The considerations discussed above were taken into account during the design of these simulations. Since surface roughness was shown to have a measurable effect on C_l and C_d, it was added to the ridges of both simulations with the same extents and roughness height as the casting, except for on the lower surface ridge of the simple-geometry simulation where a smaller roughness height was used. $C_{l,max}$ of each simulation was found to be in good agreement with the full-scale data measured by Broeren et al. (Fig. 24). C_d of the sub-scale simulations was slightly higher at low angles of attack than the casting, but agreed reasonably well at higher angles of attack. The disagreement at low angles was likely caused by significant three-dimensionality of the lower surface ridge, which was difficult to represent appropriately with 2-D simulations. Also, the height of the ridge on the lower surface was much less than the ridge on the upper surface and it is likely that this ridge behaved as a short ridge, discussed in the next section.

Short Ridges

As the name implies, short ridges tend to have smaller heights than tall ridges, but the real distinction between the two types of ridges is determined by the effect of the ridge on the airfoil pressure distribution. Broeren et al.[9] describe short ridges as generating short, stable separation bubbles which do not grow with angle of attack and have only a local effect on the airfoil pressure distribution. This is illustrated in Fig. 22, which compares the effects of short and tall ridges on the airfoil pressure distribution. The short upper surface ridge for which the pressure distribution is shown is located at x/c = 0.13, and a lower surface ridge is present at x/c = 0.15. Unlike in the case of the tall ridge, the airfoil achieves a suction peak near the airfoil leading edge of similar magnitude to that achieved when clean. The pressure distribution departs from the clean case near x/c = 0.10, just upstream of the ridge. Here, the flow rapidly decelerates before encountering the ridge, and then accelerates over the top of the ridge, similar to the case of the tall ridge. A short separation bubble is seen behind the short ridge extending from x/c = 0.15 – 0.16, and pressure recovery begins just after x/c = 0.16. This is much sooner than in the case of the tall ridge. Also notice that the C_p distribution of the short ridge matches up with the clean airfoil C_p distribution downstream of x/c = 0.20, and the trailing-edge pressure is the same in both the clean and iced-cases. The short ridge significantly altered the airfoil pressure distribution only from x/c = 0.10 to x/c = 0.20; it had only a local effect on the flowfield. Broeren et al. note that the ridge height k/c can not be used alone to determine if a ridge is a short ridge or a tall ridge. Other

factors, such as ridge shape and surface location, as well as airfoil geometry, affect the type of separation bubble generated and must also be considered.

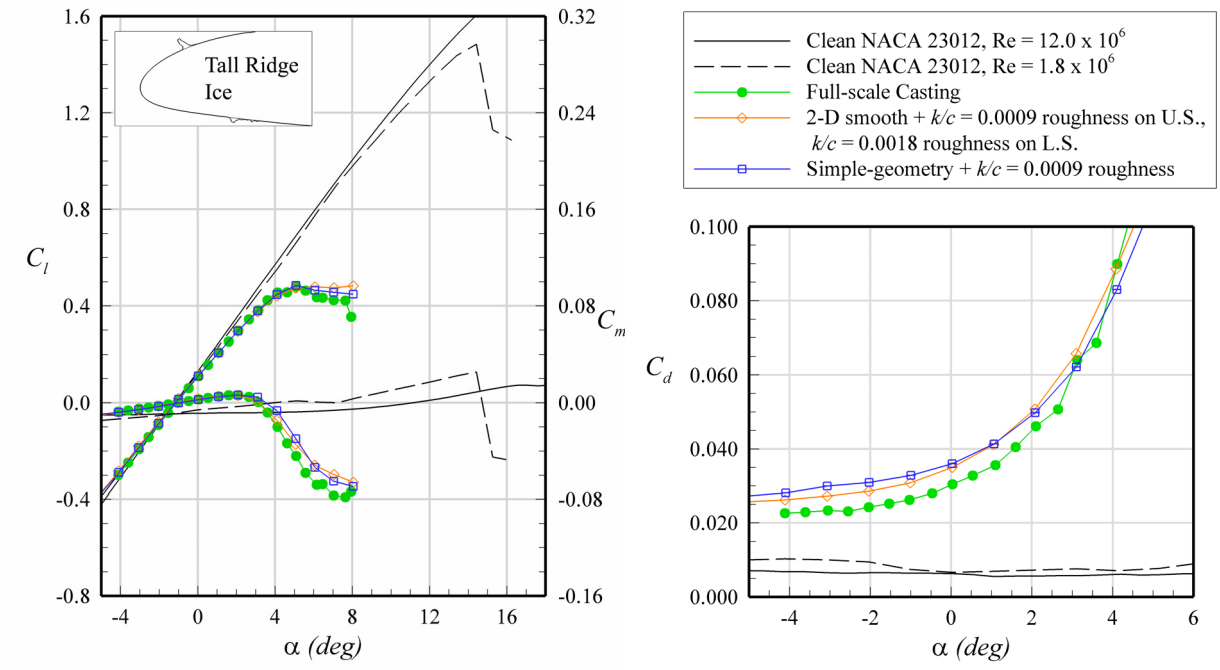

Fig. 24 Comparison of aerodynamic performance of sub-scale tall spanwise-ridge ice simulations at Re = 1.8 x 10^6 and M = 0.18 with the corresponding full-scale casting at Re = 12.0 x 10^6 and M = 0.20.[6]

Important geometric features

As with tall ridges, $C_{l,max}$ of airfoils with short ridges tends to decrease as ridge height increases for a given ridge cross-sectional geometry. Whalen[15] showed this to be true for k/c = 0.0035 – 0.0069 ridges with rectangular cross sections on a NACA 3415 airfoil, and Busch[34] for ridge heights of k/c = 0.007 and 0.009 on a NACA 23012 airfoil (also using ridges with rectangular cross-sections). However, short ridges have an increased sensitivity to cross-sectional geometry relative to tall ridges, which may be represented with simple-geometry simulations with good accuracy.[6] Busch[34] attempted to use a simple-geometry simulation with a rectangular cross-section and a 2-D smooth simulation to represent a short ridge on a NACA 23012 airfoil (Fig. 25(a)). The cross-section of the 2-D smooth simulation was representative of the cross-section of a short ridge casting at the spanwise station at which pressure taps were installed. Tracings of the ridge-ice casting were also taken at two additional spanwise stations and are shown in Fig. 25(b). Comparisons of C_l, C_m, and C_d between the two simulations and the casting are shown in Fig. 26, with all data at Re = 1.8 x 10^6 and M = 0.18 on an 18-inch chord airfoil model. The 2-D smooth simulation has $C_{l,max}$ reasonably close to that of the casting, but stalled at a 2 deg. lower angle of attack. The simple-geometry simulation, on the other hand, stalled much earlier and had a much lower $C_{l,max}$. Neither simulation modeled C_d of the casting particularly well except at low positive angles of attack. Various sizes of surface roughness were added to the 2-D simulations and were determined to decrease $C_{l,max}$ and increase C_d but did not improve simulation fidelity It is evident from this study that the cross-sectional geometry of the ridge is important to model appropriately.

Sub-scale simulation with full-scale validation

Broeren et al.[9] recently acquired aerodynamic performance data for a 72-inch chord NACA 23012 airfoil with a short ridge ice casting at Re = 12.0 x 10^6 and M = 0.20 and quantified the accuracy of sub-scale simulation techniques for this type of accretion. Since the ridge happened to have a cross-sectional geometry that was close to rectangular, a simple-geometry simulation with the same height and chordwise extent was reasoned to be a representative geometry. Previous research on small ridges had not provided consistent data on the effect of surface roughness, so the simple-geometry simulation was tested both with and without surface roughness. Two types of surface roughness were applied: standard grit roughness and simulated rivulets. Both types of roughness had the

same chordwise extents and similar *k/c* as was measured on the casting. The aerodynamic performance of selected sub-scale simulations on an 18-inch chord NACA 23012 airfoil at Re =1.8 x 10^6 and M = 0.18 is shown in Fig. 27. In the figure, three simulations are compared with the NG0671 full-scale short ridge-ice casting: SG-US, which was a simple-geometry simulation of the upper surface ridge only; SG-US & SG-LS, which was a simple-geometry simulation of both the upper and lower surface ridges; and SG+R-US & SG+R-LS, which was a simple-geometry simulation of both the upper and lower surface ridges with grit surface roughness applied. These data show that a simple-geometry simulation without roughness had $C_{l,max}$ very similar to the casting, regardless of whether the lower surface horn was simulated, but stalled more abruptly The addition of grit surface roughness caused $C_{l,max}$ to drop markedly. Applying simulated rivulets (not shown) also caused $C_{l,max}$ to decrease, though not as much. Therefore, roughness does not appear to improve the comparison of $C_{l,max}$ between the casting and simulations, consistent with the results found by Busch.[34]

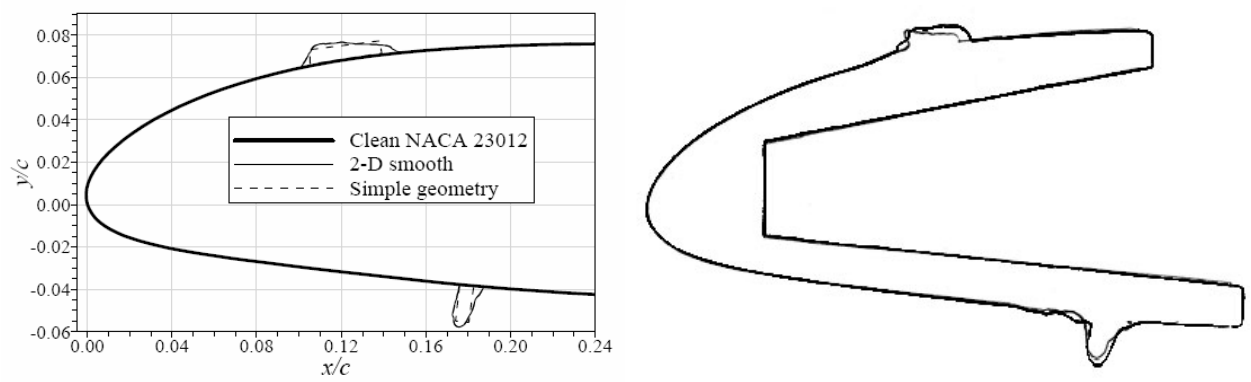

Fig. 25 Comparison of (a) 2-D smooth and simple-geometry simulations of a short spanwise-ridge ice accretion[35] and (b) tracings of the same ridge-ice accretion at two additional spanwise stations.[34]

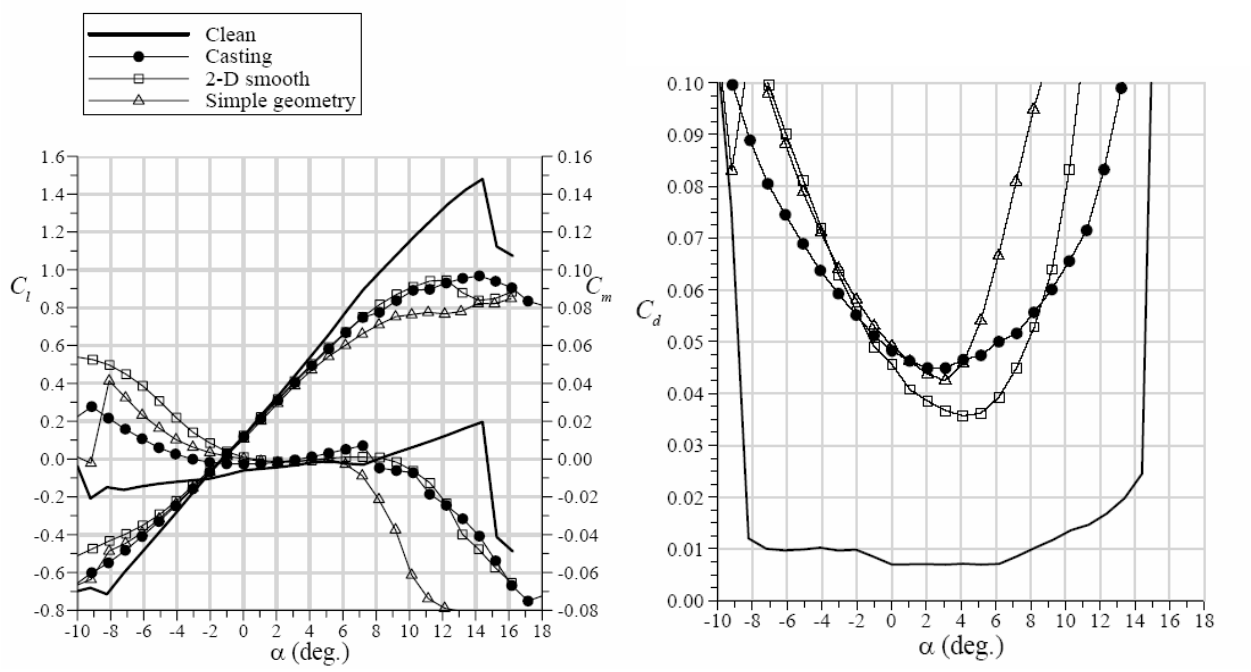

Fig. 26 Comparison of aerodynamic performance among a short ridge casting and 2-D smooth, and simple-geometry simulations.[35]

The trends in C_d were consistent with those observed for $C_{l,max}$. The two simple-geometry simulations without roughness had very similar C_d to each other and to the casting at high angle of attack, while the simulation with roughness had higher C_d than the casting at all angles of attack. Notice that the simulation of the lower-surface ridge

only affected C_d at low angles of attack; this is consistent with previous research on other types of accretion which has shown that lower surface ice accretion tends to have the most impact at low angle of attack and minimal impact at high angle of attack.[34,36]

Broeren et al.[9] show that Reynolds number effects on short spanwise ridges are small over the range Re = 4.6 x 10^6 – 15.9 x 10^6, but note that Reynolds number effects are important on this type of accretion over a range of 1.0 x 10^6 – 1.8 x 10^6. Also, the sensitivity of the short ridge-ice simulations to geometric details such as surface roughness suggests that Reynolds number effects may not be negligible. Unfortunately, no data exists for identical short spanwise ridge accretion (or simulation) geometries at Reynolds numbers from 1.8 x 10^6 – 4.6 x 10^6, so it is not known how much of the performance difference observed between the sub-scale simulation and full-scale casting aerodynamic performance is due to differing geometry or Reynolds number effects.

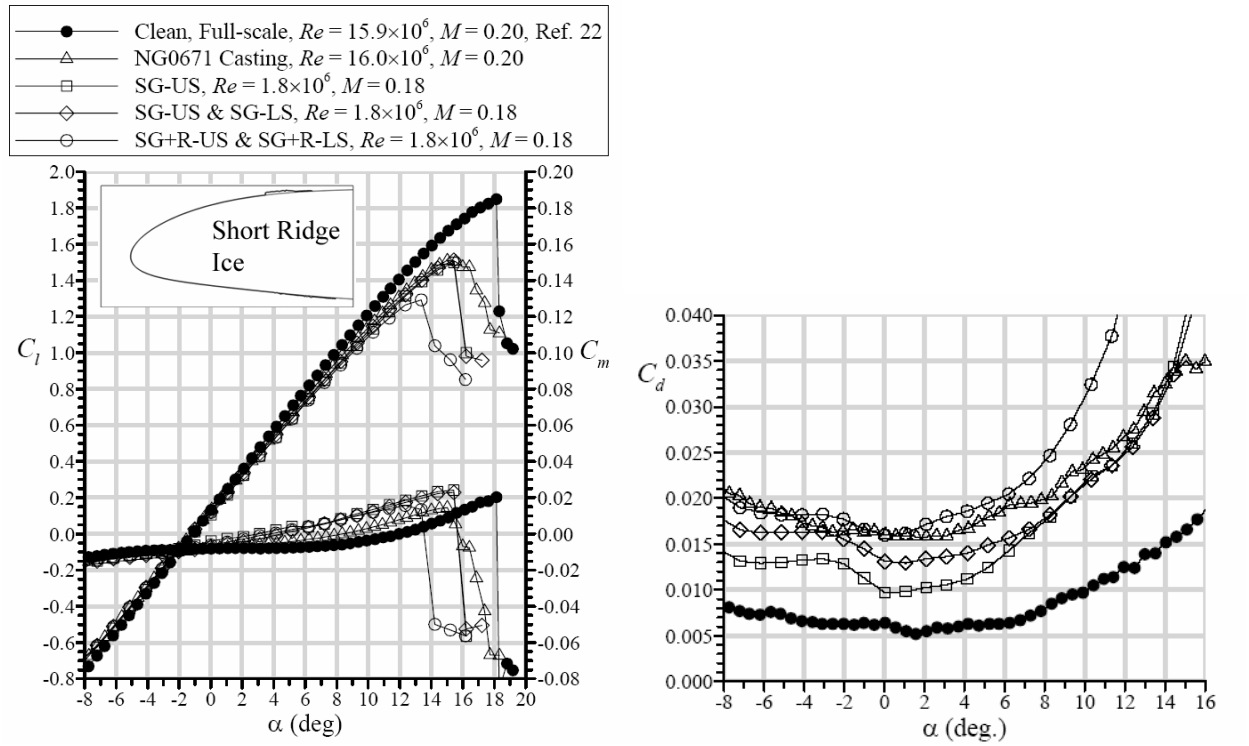

Fig. 27 Comparison of aerodynamic performance of sub-scale short spanwise-ridge ice simulations at Re = 1.8 x 10^6 and M = 0.18 with the corresponding full-scale casting at Re = 15.9 x 10^6 and M = 0.20.[9]

Conclusions

This paper discusses issues relevant to sub-scale ice accretion aerodynamic simulation. The flowfields of several types of ice accretion are briefly reviewed and important geometric features discussed. The paper addresses general issues to be considered when using sub-scale methods, and also issues specific to particular types of ice accretion. It was shown that Reynolds number effects on iced airfoils were small for Reynolds numbers greater than 4.6 x 10^6. However, for ice roughness, streamwise ice, and short ridge ice, little data exists for Reynolds numbers from 2.0 x 10^6 – 5.0 x 10^6, and the data that does exist suggests that there may be an increased dependence in this range. Further research on Re effects in this range for these types of ice accretion is recommended.

Uncertainties in ice accretion geometry should be considered when using sub-scale methods, as variations in $C_{l,max}$ on the order of 13-18% and even larger variations in C_d may result from icing tunnel repeatability issues or using tracings taken at different spanwise stations. Also, uncertainties exist in aerodynamic measurement procedures due to issues such as pressure tap placement and C_d measurement procedures. If C_d is measured using standard wake survey techniques, then C_d should be measured at multiple spanwise stations and averaged to obtain a representative value, as variations in C_d as high as 45% have been measured at different spanwise stations behind an ice simulation.

Issues specific to particular types of ice accretion are as follows:

- Ice Roughness – Important features to represent in a simulation are roughness height, concentration, and chordwise extents. Geometric scaling of ice roughness has resulted in conservative estimates of aerodynamic performance in past simulations. It is possible that this may be Reynolds number related, as Re effects appear to become more significant below Re = 3.5 x 10^6 .

- Streamwise Ice – Important features to represent in a simulation are a modification of the airfoil leading-edge geometry. The exact geometry and size of the gross shape are less important than the presence of ice at the leading edge which changes the airfoil geometry. Surface roughness has a large effect on streamwise-ice aerodynamics, but was shown to yield conservative performance estimates, perhaps because of Reynolds number effects similar to those which may be present for ice roughness accretions. When constructing a 2-D smooth simulation of a tracing of a streamwise-ice accretion, care must be taken not to two-dimensionalize highly three-dimensional features such as ice feathers.

- Horn ice – Important features to represent in a simulation are horn height, angle, location, and in some cases, tip radius. 2-D smooth horn-ice simulations have been shown to appropriately reproduce horn-ice C_l and C_d with no additional surface roughness. To reproduce the flowfield of a horn-ice accretion, spanwise variation in horn geometry or the addition of grit roughness may be necessary.

- Spanwise-ridge ice – Spanwise-ridge ice consists of two types of ridges, tall ridges and short ridges, and each requires different simulation techniques. Simulations of tall ridges should represent ridge height, location, and surface roughness; 2-D smooth and simple-geometry simulations with roughness are adequate for this type of accretion. Simulations of short ridges should represent ridge height, location, and geometry. Previous research on short ridge simulations has shown that appropriately designed simple-geometry short ridge simulations can provide reasonable estimates of the full-scale iced airfoil C_l and C_d. Adding geometrically-scaled surface roughness to such a simulation resulted in conservative estimates of aerodynamic performance. As with ice roughness, it is possible that Reynolds number effects from Re = 2.0 - 4.6 x 10^6 may be significant, but no data currently exist for short spanwise ridges in this range.

Acknowledgments

The authors wish to thank Gene Addy and Andy Broeren from NASA Glenn Research Center, Sam Lee from ASRC Aerospace Corp., and Ed Whalen from The Boeing Company for their helpful advice during this investigation. Thanks also go to Austin Ellis and the Aerospace Engineering Department Machine Shop at the University of Illinois for their assistance with this study.

References

[1] Busch, G., Broren, A., and Bragg, M., "Aerodynamic Simulation of a Horn-Ice Accretion on a Subscale Model," *J. Aircraft*, v. 45, n. 2, 2008, pp. 604-613.

[2] Bragg, M., Broeren, A., Addy, H., Potapczuk, M., Guffond, D., and Montreuil, E., "Airfoil Ice-Accretion Aerodynamics Simulation," AIAA Paper 2007-0085, *45th AIAA Aerospace Sciences Meeting & Exhibit*, Reno, NV, Jan. 2007.

[3] Bragg, M. B., Broeren, A. P., and Blumenthal, L. A., "Iced-Airfoil Aerodynamics," *Progress in Aerospace Sciences*, Vol. 41, 2005, pp. 323-362.

[4] Cummings, M.J., "Airfoil Boundary-Layer Transition Due to Large Isolated 3-D Roughness Elements in a Favorable Pressure Gradient," M.S. Thesis, Dept. of Aeronautical and Astronautical Engineering, Univ. of Illinois, Urbana, IL, 1995.

[5] Broeren, A.P. Bragg, M.B., Addy, Jr., H.E., Lee, S., Moens, F., and Guffond, D., "Effect of High-Fidelity Ice Accretion Simulations on the Performance of a Full-Scale Airfoil Model," AIAA-2008-0434, *46th Aerospace Sciences Meeting & Exhibit*, Reno, NV, Jan. 2008.

[6] Busch, G., Broeren, A., and Bragg, M., "Aerodynamic Fidelity of Sub-Scale Two-Dimensional Ice Accretion Simulations," AIAA-2008-7062, *26th AIAA Applied Aerodynamics Conference*, Honolulu, HI, Aug. 2008.

[7] Wright, W. B., "Validation Results for LEWICE 3.0," NASA CR-2005-213561, AIAA-2005-1243, Jan. 2005.

[8] Lee, S., Ratvasky, T.P., Thacker, M., and Barnhart, B.P., "Geometry and Reynolds-Number Scaling on an Iced Business-Jet Wing," AIAA-2005-1066, *43rd* AIAA Aerospace Sciences Meeting & Exhibit, Reno, NV, Jan. 2005.
[9] Broeren, A.P., Whalen, E.A., Busch, G.T., and Bragg, M.B., "Aerodynamic Simulation of Runback Ice Accretion," AIAA-2009-4261, *1st AIAA Atmospheric & Space Environments Conference*, San Antonio, TX, Jun. 2009.
[10] Broeren, A. P., Bragg, M. B., "Effect of Airfoil Geometry on Performance with Simulated Intercycle Ice Accretions," AIAA-2003-0728, 2003.
[11] Broeren, A. P., Addy, Jr., H. E., Bragg, M. B., "Effect of Intercycle Ice Accretions on Airfoil Performance," AIAA-2002-0240, *40th Aerospace Sciences Meeting & Exhibit*, Reno, NV, Jan. 2002.
[12] Tsao, J. and Anderson, D.N., "Further Assessment of MVD Effects in SLD Applications," AIAA-2005-0072, *43rd AIAA Aerospace Sciences Meeting & Exhibit*, Reno, NV, Jan. 2005.
[13] Tsao, J. and Anderson, D.N., "Results of Scaling Tests for Large Model-Size Ratios," AIAA-2006-0467, *44th AIAA Aerospace Sciences Meeting & Exhibit,* Reno, NV, Jan. 2006.
[14] Whalen, E.A., Broeren, A. P., and Bragg, M.B., "Considerations for Aerodynamic Testing of Scaled Runback Ice Accretions," AIAA-2006-0260, *44th AIAA Aerospace Sciences Meeting & Exhibit,* Reno, NV, Jan. 2006.
[15] Whalen, E.A., "Aerodynamics of Runback Ice Accretions," Ph.D. Dissertation, Dept. of Aerospace Eng., Univ. of Illinois, Urbana, IL, 2007.
[16] Gurbacki, H. M., "Ice-Induced Unsteady Flowfield Effects on Arifoil Performance," Ph. D. Dissertation, Dept. of Aeronautical and Astronautical Engineering, Univ. of Illinois, Urbana, IL, 2003.
[17] Addy, Jr., H. E., and Chung, J. J., "A Wind Tunnel Study of Icing Effects on a Natural Laminar Flow Airfoil," AIAA-2000-0095, 38th Aerospace Sciences Meeting and Exhibit, NV, Jan. 2000.
[18] Addy, Jr., H. E., Broeren, A. P., Zoeckler, J. G., and Lee, S., "A Wind Tunnel Study of Icing Effects on a Business Jet Airfoil," AIAA Paper 2003-0727, 41st Aerospace Sciences Meeting and Exhibit, Reno, NV, Jan. 2003.
[19] Blumenthal, L. A., Busch, G. T., Broeren, A. P., and Bragg, M. B., "Issues in Ice Accretion Aerodynamic Simulation on a Sunscale Model," AIAA-2006-262, *44th AIAA Aerospace Science Meeting & Exhibit*, Reno, NV, Jan. 2006.
[20] Jackson, D. G., "Effect of Simulated Ice and Residual Ice Roughness on the Performance of a Natural Laminar Flow Airfoil," M.S. These, Dept. of Aeronautical and Astronautical Engineering, Univ. of Illinois, Urbana, IL, 1999.
[21] Shin, J., and Bond, T.H., "Results of an Icing Test on a NACA 0012 Airfoil in the NASA Lewis Icing Research Tunnel," AIAA Paper-92-0647, 1992.
[22] Shin, J., and Bond, T.H., "Repeatability of Ice Shapes in the NASA Lewis Icing Research Tunnel," *J. Aircraft*, V. 31, n. 5, 1994, pp. 1057-1063.
[23] Miller, D.R., Potapczuk, M.G., and Langhals, T.J., "Preliminary Investigation of Ice Shape Sensitivity to Parameter Variations," AIAA-2005-0073, *43rd AIAA Aerospace Sciences Meeting & Exhibit,* Reno, NV, Jan. 2005.
[24] Addy, H.E., Potapczuk, M.G., and Sheldon, D.W., "Modern Airfoil Ice Accretions," AIAA-1997-0174, *35th AIAA Aerospace Sciences Meeting & Exhibit,* Reno, NV, Jan. 1997.
[25] Blumenthal, L. A., "Surface Pressure Measurement on a Three-Dimensional Ice Shape," M.S. Thesis, Dept. of Aerospace Engineering, Univ. of Illinois, Urbana, IL, 2005.
[26] Busch, G., Broeren, A., and Bragg, M., "Aerodynamic Simulation of a Horn-ice Accretion on a Subscale Model," AIAA 2007-87, *45th AIAA Aerospace Sciences Meeting & Exhibit*, Reno, NV, Jan. 2007.
[27] Guglielmo, J. J., and Selig, M. S., "Spanwise Variations in Profile Drag for Airfoils at Low Reynolds Numbers," *J. Aircraft*, Vol. 33, No. 4, 1996, pp. 699-707.
[28] Althaus, D., "Drag Measurements on Airfoils," OSTIV Congress, Paderborn. Germany, 1981.
[29] Bragg, M. B., Khodadoust A., and Spring, S. A., "Measurements in a Leading-Edge Separation Bubble Due to a Simulated Airfoil Ice Accretion," AIAA J Vol. 30, No. 6, 1992, pp. 1462-1467
[30] Brumby, R. E., "Wing Surface Roughness – Cause & Effect," D. C. Flight Approach, Jan. 1979, pp. 2-7.
[31] Brumby, R.E., "The Effect of Wing Ice Contamination on Essential Flight Characteristics," AGARD CP-496, 1991, pp. 2.1–2.4.
[32] Papadakis, M. and Gile Laflin, B.E., "Aerodynamic Performance of a Tail Section with Simulated Ice Shapes and Roughness," AIAA-2001-0539, *39th AIAA Aerospace Sciences Meeting & Exhibit*, Reno, NV, Jan. 2001.

[33] Papadakis, M., Yeong, H.W., Chandrasekharan, R., Hinson, M., Ratvasky, T., "Effects of Roughness on the Aerodynamic Performance of a Business Jet Tail," AIAA-2002-0242, *40th AIAA Aerospace Sciences Meeting & Exhibit*, Reno, NV, Jan. 2002.
[34] Busch, G. T., "Ice Accretion Aerodynamic Simulation on a Subscale Model," M.S. Thesis, Dept. of Aerospace Engineering, Univ. of Illinois, Urbana, IL, 2006.
[35] Broeren, A. P., Busch, G. T., and Bragg, M. B., "Aerodynamic Fidelity of Ice Accretion Simulation on a Subscale Model," SAE Paper 2007-01-3285, 2007.
[36] Kim, H., "Effects of Leading-Edge Ice Accretion Geometry on Airfoil Performance," M.S. Thesis, Dept. of Aerospace Engineering, Univ. of Illinois, Urbana, IL, 2004.
[37] Jacobs, J. J., "Iced Airfoil Separation Bubble Measurements by Particle Image Velocimetry," Ph. D. Dissertation, Dept. of Aerospace Engineering, Univ. of Illinois, Urbana, IL, 2007.
[38] Jacobs, J. J., and Bragg, M. B., "Particle Image Velocimetry Measurements of the Separation Bubble on an Iced Airfoil," AIAA-2006-3646, *24th Applied Aerodynamics Conference*, San Francisco, CA, Jun. 2006.
[39] Gurbacki, H. M., and Bragg, M. B., "Unsteady Flowfield About an Iced Airfoil," AIAA-2004-0562, *42nd Aerospace Sciences Meeting and Exhibit*, Reno, NV, Jan. 2004.
[40] Papadakis, M., Alansatan, S., Seltmann, M., "Experimental Study of Simulated Ice Shapes on a NACA 0011 Airfoil," AIAA-99-0096, *37th AIAA Aerospace Sciences & Exhibit*, Reno, NV Jan. 1999.
[41] Broeren, A.P., Lee, S., LaMarre, C.M., and Bragg, M.B., "Effect of Airfoil Geometry on Performance with Simulated Ice Accretions Volume 1: Experimental Investigation," Report No. DOT/FAA/AR-03/64, August 2003.
[42] Kim, H.S. and Bragg, M.B., "Effects of Leading-edge Ice Accretion Geometry on Airfoil Performance," AIAA-99-3150, *17th AIAA Applied Aerodynamics Conference*, Norfolk, VA, Jun. 1999.
[43] Papadakis, M., Gile Laflin, B.E., Youssef, G.M., Ratvasky, T.P., "Aerodynamic Scaling Experiments with Simulated Ice Accretions," AIAA-2001-0833, *39th AIAA Aerospace Sciences Meeting & Exhibit*, Reno, NV, Jan. 2001.
[44] Lee, S., "Effects of Supercooled Large-Droplet Icing on Airfoil Aerodynamics," Ph. D. Dissertation, Dept. of Aeronautical and Astronautical Engineering, Univ. of Illinois, Urbana, IL, 2001.
[45] Lee, S., and Bragg, M.B., "Experimental Investigation of Simulated Large-Droplet Ice Shapes on Airfoil Aerodynamics," *Journal of Aircraft*, Vol. 36, No. 5, Sept.-Oct. 1999, pp. 844-850.
[46] Lee, S., Kim, H. S., Bragg, M. B., "Investigation of Factors that Influence Iced-Airfoil Aerodynamics," AIAA-2000-0099, *38th AIAA Aerospace Sciences Meeting & Exhibit*, Reno, NV, Jan. 2000.
[47] Lee, S., and Bragg, M.B., "Effects of Simulated-Spanwise Ice Shapes on Airfoils: Experimental Investigation," AIAA-99-0092, *37th AIAA Aerospace Sciences Meeting & Exhibit*, Reno, NV, Jan. 1999.